

**Validation of the Leaf Area Index product from
MODIS-15 for Rice using a Soil-Leaf-Canopy
Radiative Transfer Model
A case study of Seville, Spain**

Course Title:	Geo-Information Science and Earth Observation for Environmental Modelling and Management
Level:	Master of Science (MSc)
Course Duration:	September 2008 - March 2010
Consortium partners:	University of Southampton (UK) Lund University (Sweden) University of Warsaw (Poland) International Institute for Geo-Information Science and Earth Observation (ITC) (The Netherlands)
GEM thesis number:	2010-27

Jose Alfredo Suarez Urrutia
March 2010

Validation of the Leaf Area Index product from
MODIS-15 for Rice using a Soil-Leaf-Canopy
Radiative Transfer Model
A case study of Seville, Spain

by

José Alfredo Suárez Urrutia

Thesis submitted to the International Institute for Geo-information Science and Earth Observation in partial fulfilment of the requirements for the degree of Master of Science in Geo-information Science and Earth Observation for Environmental Modelling and Management

Thesis Assessment Board

Chairman	Prof. Dr. Ir. E.M.A. Smaling
External Examiner	Prof. Dr. Hab. K. Dąbrowska-Zielińska
First Supervisor	Dr. Ir. C.A.J.M. de Bie
Second Supervisor	M.Sc. V. Venus
GEM coordinator	M.Sc. A. Kooiman



UNIVERSITY OF TWENTE.

ITC

FACULTY OF GEO-INFORMATION SCIENCE AND EARTH OBSERVATION

Disclaimer

This document describes work undertaken as part of a programme of study at the International Institute for Geo-information Science and Earth Observation. All views and opinions expressed therein remain the sole responsibility of the author, and do not necessarily represent those of the institute.

Abstract

The performance of the MODIS LAI/FPAR 8-day composite product and a physically based radiative transfer model called Soil-Leaf-Canopy (SLC) were compared to identify which was capable to perform a better estimation of LAI compared to *in situ* measurements. The study was carried out in the zone of rice production of Seville, Spain.

The performances of the MODIS product and SLC model were assessed against LAI values collected in the field using LAI-2000 during July and August of 2008. MODIS LAI/FPAR coarse resolution product (MOD15A2) was compared against *in situ* measurements using a disaggregation technique to estimate the fraction cover of vegetation based on NDVI retrievals from LANDSAT 7 ETM+ products. LAI from SLC was estimated by means of the model inversion with the aid of a look-up table and a iterative method of inversion (LUT). Forward modelling of the spectral reflectances was carried out prior to the inversion, using MODIS spectral reflectance product (MOD09A1) to adjust the outputs of the LUT. Estimated LAI was compared against *in situ* measurements to evaluate the performance of the inversion from SLC.

MODIS LAI/FPAR values showed a Pearson's correlation coefficient (R) of 0.44 against *in situ* measurements. Estimated LAI from SLC showed a Pearson's correlation coefficient of 0.50. Improvements of 10% of the estimations were observed in SLC's values compared to MODIS LAI/FPAR values. The study concludes that despite of the complex parameters required by the model, SLC's performance is better for the prediction of LAI for rice than the MODIS LAI/FPAR product. It was also observed that improvements in the method of inversion can considerable enhance the performance of SLC.

Keywords: Leaf area index (LAI), MODIS LAI/FPAR, Soil-leaf-canopy (SLC), Radiative transfer model (RTM).

Acknowledgements

First, I want to thank the Erasmus Mundus program of the European Union for granting me the opportunity to be part of GEM 2008-2010. Having been part of the program has been an unforgettable experience where academia, culture and friendship profoundly marked my life. I hope that the knowledge acquired during these 18 months, may contribute to the research and development in Guatemala, thus fulfilling one of the objectives with which the EM program was created. I also want to thank the four representatives of the GEM consortium, without whose support this vital program had been a failure: Prof. Terry Dawson, University of Southampton; Prof. Petter Pilesjo, Lund University; Prof. Katarzyna Dąbrowska-Zielińska, University of Warsaw; and Prof. Andrew Skidmore, ITC (now part of the University of Twente). I also want to thank the team (professors, lecturers and secretaries) of each of the consortium universities for the excellent work.

I express my sincere gratitude to my supervisors, Dr. Kees de Bie and M.Sc. Valentijn Venus, since they shared their knowledge and time to the successful completion of this investigation. Without his patience and guidance, this research would not have been what it is today. A special mention to M.Sc. Nguyen Ha and Prof. Wouter Verhoef, since their comments and advices during the conduct of this research were very useful.

Special thanks to my classmates, for your friendship, support and trustful believe in me as their leader on this adventure called GEM 2008-2010. I wish you success in your future life and hope someday we can meet again. In addition, a special thanks to all my ITC friends, members of the Student Association Board (SAB) and specially my Latin American friends, because during this final stage home did not feel so far away.

Last but not least, special thanks to my beloved wife Claudia, who fully supported me during these 18 months. Without her support, it would have been impossible to complete this stage successfully. To my family in Guatemala, thank you very much for your support, especially my mother Lilian Anabella who instilled in me the spirit that dreams can be achieved, if one believes and works hard with dedication.

To the Guatemalan Sugarcane Research and Training Center (CENGICANA), whose total support has been key to the completion of this stage of my life.

To God, source of inspiration, peace and love.

Table of contents

1.	Introduction.....	7
1.1.	Methods to estimate Leaf Area Index through remote sensing	7
1.2.	Radiative Transfer Models	8
1.2.1.	Soil-Leaf-Canopy radiative transfer model	9
1.3.	The MODIS LAI/FPAR product.....	10
1.3.1.	Indirect estimations of LAI in rice	12
2.	Research approach	13
2.1.	Research problem.....	13
2.2.	Research objective	13
2.3.	Research questions	13
	• Are MODIS LAI/FPAR product correlated with <i>in situ</i> measurements of LAI? 13	
	• Can estimated LAI values present a strong correlation with <i>in situ</i> measurements?.....	14
	• Can estimated LAI values improve the estimation of the index in rice compared to MODIS LAI/FPAR product values?	14
3.	Method.....	15
3.1.	Method overview	15
3.2.	Study area.....	16
3.3.	Data used.....	18
	• MODIS products	18
	• LANDSAT 7 ETM+	19
	• Orthophotos.....	19
3.4.	Quality assessment of the MODIS LAI/FPAR product	20
3.4.1.	Field data collection	20
3.4.2.	Preparation of LAI from field data	20
3.4.3.	Preparation of LAI dataset from MOD15A2.....	20
3.4.4.	Disaggregation technique for MOD15A2 product	21
3.4.5.	Comparison between measured LAI values and MOD15A2 LAI values	25
3.5.	Estimation of the LAI from the SLC radiative transfer model	25
3.5.1.	Preparation of surface reflectance dataset from MOD09A1.....	25
3.5.2.	SLC model software	25
3.5.3.	Look-up table inversion.....	26
3.5.4.	Comparison between measured values and estimated LAI from SLC	28

4.	Results.....	29
4.1.	Quality assessment of the MODIS LAI/FPAR product	29
4.1.1.	Correction of LAI measurements from field	29
4.1.2.	Comparison between LAI values from the field and MOD15A2... ..	33
4.2.	Estimation of LAI from SLC and quality assessment	36
4.3.	Comparison between estimated LAI from SLC and MOD15A2 LAI.....	38
5.	Discussion.....	40
5.1.	Quality assessment of the MODIS LAI/FPAR product	40
5.2.	Estimation of LAI from SLC and quality assessment	41
6.	Conclusions.....	42
7.	Limitations and recommendations	43
7.1.	Limitations	43
7.2.	Recommendations	43
8.	References.....	45
9.	Appendices	49
	Appendix A	49
	Appendix B	51

List of figures

Figure 1 Methodology flowchart.	16
Figure 2 Location of Seville within Andalucía. Inset: location of the autonomous community of Andalucía in Spain (Khan et al., 2010).	18
Figure 3 Overall method to solve the mixed pixel problem.	23
Figure 4 MOD15A2 pixels containing rice's sampled plots.	24
Figure 5 Behaviour of measured values as a function of time of the day.	29
Figure 6 Corrected LAI values after the transformation.	30
Figure 7 Comparison between corrected values and original values with their respective trend lines.	31
Figure 8 Comparison between original and corrected LAI.	32
Figure 9 Histogram of the corrected values of LAI measured in the field (per week).	32
Figure 10 Histogram of the MOD15A2 product.	33
Figure 11 Comparison between LAI values from the field and MOD15A2.	34
Figure 12 Scatter plot of the correlation between corrected LAI from the field and MOD15A2 LAI for the first week of the fieldwork campaign (6 th week after sowing).	35
Figure 13 Scatter plot of the correlation between corrected LAI from the field and MOD15A2 LAI for the 4 th week of the fieldwork campaign (9 th week after sowing).	35
Figure 14 Histogram of the values of LAI estimated with SLC.	36
Figure 15 Comparison between LAI from field and from SLC.	37
Figure 16 Scatter plot of the correlation between LAI from the field and from SLC for the first week of the fieldwork campaign (6 th week after sowing).	37
Figure 17 Scatter plot of the correlation between LAI from the field and from SLC for the 4 th week of the fieldwork campaign (9 th week after sowing).	38
Figure 18 Scatter plot of the estimated values of LAI and MOD15A2 LAI values. ..	39

List of tables

Table 1	Science datasets specifications for MOD15A2 product (adapted from https://lpdaac.usgs.gov/)	21
Table 2	Science datasets specifications for MOD09A1 product (adapted from https://lpdaac.usgs.gov/)	26
Table 3	Soil, leaf and canopy parameters used for the forward modelling of the surface reflectance of rice.	27

1. Introduction

Thanks to the capability to characterize land surfaces with fast and non-destructive techniques, remote sensing has become a key method for estimate indirectly biophysical vegetation variables as the Leaf Area Index (LAI) (Stroppiana et al., 2006). LAI (the total one-sided leaf area per ground surface area) is a well-known structural characteristic of the plant that has been widely used to monitor vegetation (Darvishzadeh et al., 2008b). Changes in LAI through time and space provide important information about land surface processes and how to model those processes (Qin et al., 2008). In the field of agriculture, crop physiologists and modellers have used LAI to estimate foliage cover and predict crop growth and yield (Clevers and van Leeuwen, 1996; Haboudane et al., 2004; Jinsong et al., 2007).

1.1. Methods to estimate Leaf Area Index through remote sensing

Methods to estimate LAI through remote sensing can be divided roughly in four: 1) Development of relationships between LAI and vegetation indices (VI); 2) Use of lookup tables (LUT); 3) Neural networks (NN), and 4) Inversion of physically based canopy radiative transfer models (RTM) (Liang, 2004). All methods have their strengths and weaknesses. Vegetation Indices are very simple to use, but the relationships between VI and biophysical parameters have shown be specific to the type of vegetation, site and sensor; this makes them unsuitable for application at regional scales or seasons (Colombo et al., 2003; Gobron et al., 1997). Lookup tables and neural networks proved that are very useful in inversion studies (Qin et al., 2008). Their capability to speed up the process of inversion due to computational procedures is a strength of these methods (Yi et al., 2008). However, the large number of parameters that they require makes them difficult to generalize (Qin et al., 2008). In addition, the performance of these methods depends on a training database consisting of canopy reflectance spectra and biophysical variables, which are difficult to retrieve for large geographic areas (Houborg and Boegh, 2008). Inversion of RTMs has prove its capability to predict biophysical variables in diverse studies with different types of vegetation (Darvishzadeh et al., 2008a; Kobayashi et al., 2007; Meroni et al., 2004; Yongming et al., 2004). However, the

inversion of RTMs also has the problem of the “ill posed process” (Combal et al., 2003) which leads to have similar solution for completely different canopy structures.

1.2. Radiative Transfer Models

The radiant energy that vegetation canopy transmits to the atmosphere by reflectance and complicated biophysical and biochemical processes from solar energy has been described by the three-dimensional radiative transfer equation (Ross, 1981). The equation aims to determine how environmental variables (e.g. soil background) and canopy structure (leaves, stems) influence the relationships between absorbed, transmitted and reflected radiation (Huang et al., 2007). As was mentioned above, factors and processes controlling top-of-canopy (TOC) reflectance are too numerous and complex that a simple empirical equation cannot explain. For that matter, Ross’s three-dimensional radiative transfer equation - translated in radiative transfer models (RTM) - provide an explicit connection between the biophysical variables of the canopy, the view and illumination geometry with the canopy reflectance (Koetz et al., 2005). However, by nature, a RTM provides values of reflectance from biophysical variables, which leads us to the need of invert the model in order to retrieve biophysical variables from reflectance values. The inversion of RTM provides a method to recalibrate the model by optimization techniques using well known variables of the canopy (Weiss et al., 2001).

One weakness of the RTMs inversion is that by nature the inversion is an “ill-posed process” (Combal et al., 2003). The characteristics of method may lead to similar solutions and reflectance values for completely different canopy structures. To reduce the effect of the inversion, prior information should be consider before modelling: a) Ancillary data measured on site or products from another sensor, b) Knowledge about the canopy architecture to define the class of RTM to be used and c) Knowledge of typical distribution of canopy biophysical variables to be used as an input in the RTM (Combal et al., 2003). This prior information may lead to a strong process of modelling and better results of the method.

Some of the most common RTMs used in research are PROSPECT (Jacquemoud and Baret, 1990), Scattering by Arbitrary Inclined Leaves (SAIL) (Verhoef, 1984), modified versions of them like 4SAIL2 (Verhoef and Bach, 2007) or the combination of both like PROSAIL (PROSPECT + SAIL) (Bacour et al., 2002). However, like any other models, PROSPECT and SAIL have their own weaknesses.

SAIL has a low capacity to simulate heterogeneous canopies (clumping at several scales) and PROSPECT requires to be combined with other RTM to applications at canopy level (PROSPECT development is based on leaf level applications) (Feret et al., 2008).

1.2.1. Soil-Leaf-Canopy radiative transfer model

A recent developed RTM model called Soil-Leaf-Canopy or SLC (Verhoef and Bach, 2007), integrates a modified soil bidirectional reflectance distribution function (BRDF) model (Hapke, 1981), a robust version of the PROSPECT leaf optical properties model (Jacquemoud and Baret, 1990), and the canopy radiative transfer model 4SAIL2 -a robust version of SAIL with hot spot effect- (Verhoef, 1984). Because the use of a BRDF model instead of the Lambertian soil background used in PROSAIL, the model is described as suitable for a broad variety of soil-vegetation objects. In addition, the canopy part of the model (4SAIL2) considers vertical heterogeneities in the form of leaf colour gradients and horizontal heterogeneities related to crown clumping as well, which leads to realistic results with a minimum number of parameters (Verhoef and Bach, 2007). The model has been validated in bare soil, maize and forest with CHRIS-PROBA data in Germany during 2005 and 2006. However, a formal model inversion and accuracy assessment was not achieved due to the lack of ground truth data (Verhoef and Bach, 2007).

The integration of the three models is what makes SLC a suitable tool for the evaluation of the model that NASA uses to generate the MOD15A2 product. The radiative transfer model used by NASA considers the soil anisotropy, non-Lambertian surfaces and canopy 3D effects to simulate canopy spectral response of vegetation (Knyazikhin et al., 1998). The incorporation of the BRDF (non-Lambertian) effect in Hapke's model and the consideration of the vertical and horizontal heterogeneity in canopy of 4SAIL2 (3D effect) provide the tools to simulate the canopy spectral response in similar way as the NASA radiative transfer model does.

In addition, is important to mention that SLC's library contains information about spectral responses for different water-cover backgrounds, which is expected to improve considerably the performance of the RTM due to the particular characteristics of rice's growth.

1.3. The MODIS LAI/FPAR product

The launch of TERRA platform with the moderate resolution imaging spectroradiometer (MODIS) generated a new opportunity to develop vegetation-based products, due to the increase of spectral radiance to be sampled from the sensor. One of the products that has been developed is the MODIS LAI/FPAR product, which is being produced operationally and is available free of charge. The product uses an algorithm based in a stratification of six biomes: grasses and cereal crops, shrubs, broadleaf crops, savannas, broadleaf forests and needle forests (Myneni et al., 2002). Therefore, the vegetation that could be of interest for a specific purpose is considered (according to the algorithm) as one of these six biomes.

The algorithm consists of a main procedure that exploits the spectral information content of MODIS surface reflectance at up to seven spectral bands. Should this main algorithm fail, a back-up algorithm is triggered to estimate LAI and FPAR using vegetation indices. The algorithm requires a land cover classification that is compatible with the radiative transfer model used in the derivation of the product. Such a classification based on vegetation structure was proposed and it is expected to be derived from the MODIS Land Cover Product (Knyazikhin et al., 1999).

- **Derivation techniques and algorithm**

The algorithm for retrieving the LAI and FPAR from atmospherically corrected BRDF, compares observed and modelled canopy reflectance for a suite of canopy structures and soil patterns that represents a range of expected natural conditions. The algorithm is based on the formulation of the inverse problem that the sun and view directions, BRDFs, N spectral bands and uncertainties are given. All acceptable solutions are the ones where all canopy and soil patterns differ from the modelled and observed BRDF. This difference should be equivalent or less than the corresponding uncertainty to be considered as a solution. If the problem has a unique solution for a given set of surface reflectances, the mean LAI coincides with this solution and its dispersion equals zero. If the problem has multiple solutions, the algorithm provides a weighted mean calculated in accordance with the frequency of the occurrence of LAI. The dispersion magnitude indicates the reliability of the corresponding LAI value. The accuracy of retrievals cannot be improved if additional information is not available. It is important to mention that canopy properties, soil patterns, leaf optical properties and solutions of the inverse problem are stored in the form of a Look-up-Table (LUT) which then is used routinely to

identify patterns of canopy reflectances as a function of canopy structure and soil type (Myneni et al., 2003). The mentioned approach provides convergence of the algorithm because if more of the spectral information is available, the more reliable and accurate the algorithm output will be (Wang et al., 2001).

In the case of a fail in the algorithm due to pixel corruption, a back-up algorithm is triggered to estimate LAI and FPAR using vegetation indices. Empirical MODIS specific NDVI-LAI and NDVI-FPAR relationships are expected to be derived from MODIS LAI and FPAR fields and MODIS Surface Reflectance Product (Myneni et al., 2003)

- **Applications**

There are some discrepancies concerning the quality of the information of the MODIS LAI/FPAR products compared to *in situ* measured values of LAI. A study of validation of the MODIS LAI/FPAR product carried out in four different sites indicated that because of the nature of the algorithm (non-linear), it will always underestimate the retrieved LAI from coarse resolution reflectance data (Tian et al., 2002). On the other hand, a study carried out in semi-arid regions of Senegal during 2001 and 2002, showed that the MODIS LAI product had an overestimation between 2 – 15% compared to *in situ* measurements (Fensholt et al., 2004). These discrepancies about the quality of the MODIS LAI/FPAR product are evident and related to the characteristics of the biome where the studies were carried out. Another cause of the discrepancies could be to the changes in land cover, which affects directly in the assignation of the biome. Collection 5 of the product has shown improvements in the algorithm, mainly in the estimation of LAI in woody vegetation. Some of these improvements are due to the use of the combination of the MODIS sensors (Terra and Aqua) (Yang et al., 2006). However, further research is necessary to evaluate the level of these improvements, specifically in grasslands and cereal crops biomes.

As mentioned before, use of remote sensing for estimation of biophysical variables like LAI has become an alternative for the traditional destructive methods. These indirect methods, which measure the radiation transmitted through the canopy, are widely in use (Stroppiana et al., 2006). Estimations of LAI from spectral reflectance measurements have shown promising results, especially where the index is needed to model crop growth. Studies specifically on rice are yet to be done.

1.3.1. Indirect estimations of LAI in rice

Due to its special characteristics of growing in flooded fields, the estimation of rice's biophysical variables requires a modified approach. The layer of water on the soil modifies considerably the spectral reflectance of the soil-plant system. In addition, the crop stage must be considered when estimating LAI. The dynamics of the rice fields are characterized in three stages: a) flooding and transplanting stage; b) growing stage; and c) fallow stage after harvest. In the first stage, the surface is a mixture of water (depths between 2 and 15 cm) and rice plants. During the growing stage, the canopy of the crop covers most of the surface area. Before the third stage, the surface changes again, due to the decrease of the moisture in the crop and the decrease of the number of leaves (Xiao et al., 2006). These considerations are the ones that pose challenges for the remote sensing analysis in the crop: presences of a fluctuate background with the proper dynamic of the crop.

In 2006, MODIS LAI/FPAR product was assessed in rice and it showed differences in the estimation of LAI compared to field measurements. The differences were bigger in booting, heading and milking stages and smaller in tiller and maturing stages (Wu et al., 2006). Since that time, model adjustments are still unknown.

2. Research approach

2.1. Research problem

The Leaf Area Index (LAI) is a key biophysical parameter of vegetation for the estimation of relationships between soil-plant-atmosphere. In the field of the agriculture, LAI has been used as an input in crop models to predict growth and yield. Before the era of remote sensing, common methods to measure LAI were destructive and time-consuming. Nowadays, the development of new remote sensing technologies provided new perspectives to estimate LAI. The MODIS LAI/FPAR product has been widely used at a global scale. Despite of the improvements in the MODIS LAI/FPAR algorithm (Collection 5), it is believed that the product still has a lack of quality information for specific crop modelling purposes. This lack of quality could obey to the implications of the use of MODIS land cover product as an input of the algorithm for six general biomes. Another reason for this lack of quality could be the coarse resolution of the pixel (approx. 1 km) which is considerably bigger than agricultural plots. Moreover, this lack of quality should be more evident in the case of rice because the floodwater where the crop grows affects the spectral reflectance. The estimation of rice LAI from remote sensed data, requires the study of a radiative transfer model, specifically Soil-Leaf-Canopy (SLC). Generate trustful information of rice's LAI with more precision than MODIS LAI/FPAR product and in concordance with *in situ* measurements, will help crop modellers to predict growth and yield of the crop.

2.2. Research objective

Assess the use of MODIS hyper-temporal data to estimate Leaf Area Index of rice during the vegetative stage, using a Soil-Leaf-Canopy (SLC) radiative transfer model (RTM).

2.3. Research questions

- Are MODIS LAI/FPAR product correlated with *in situ* measurements of LAI?

- Can estimated LAI values present a strong correlation with *in situ* measurements?

H₀: Estimated values of LAI explain less than 75% of the variation of *in situ* measurements.

H₁: Estimated values of LAI explain more than 75% of the variation of *in situ* measurements.

- Can estimated LAI values improve the estimation of the index in rice compared to MODIS LAI/FPAR product values?

H₀: Estimated values of LAI will improve less than 15% the performance of MODIS LAI/FPAR product values.

H₁: Estimated values of LAI will improve more than 15% the performance of MODIS LAI/FPAR product values.

3. Method

3.1. Method overview

The research's progress could be summarized into three main procedures according to the flowchart presented in the Figure 1:

- Quality assessment of the MODIS LAI/FPAR product based on *in situ* measurements (Figure 1a).
- Estimation of LAI from the Soil-Canopy-Leaf radiative transfer model (Figure 1b), and quality assessment based on *in situ* measurements.
- Comparison of the performances of the LAI from the MOD15A2 product and the LAI estimated from the SLC model (Figure 1c).

The quality assessment of the MODIS LAI/FPAR (MOD15A2) product consisted in the comparison between LAI values measured in the field and LAI values from 8-day composite images of the MOD15A2 product using correlations. A disaggregation method using NDVI were used to reduce the effect of the mixed pixel in the MOD15A2 product.

The estimation of the LAI from the SLC model involved four steps: a) the generation of look-up tables (LUT) which contained modelled spectral signatures of the crop; b) the adjustment of the modelled spectral signatures of the SLC model with the spectral signatures of the MODIS surface reflectance product (MOD09A1); c) the estimation of LAI from the adjusted spectral signatures of the RTM; and d) the comparison between estimated LAI from SLC model against *in situ* measurements by means of the use of correlations.

A final step consisted in the comparison of the performances of the MODIS LAI/FPAR product against the estimated LAI from the SLC. Correlation coefficients calculated for both procedures were compared for this purpose.

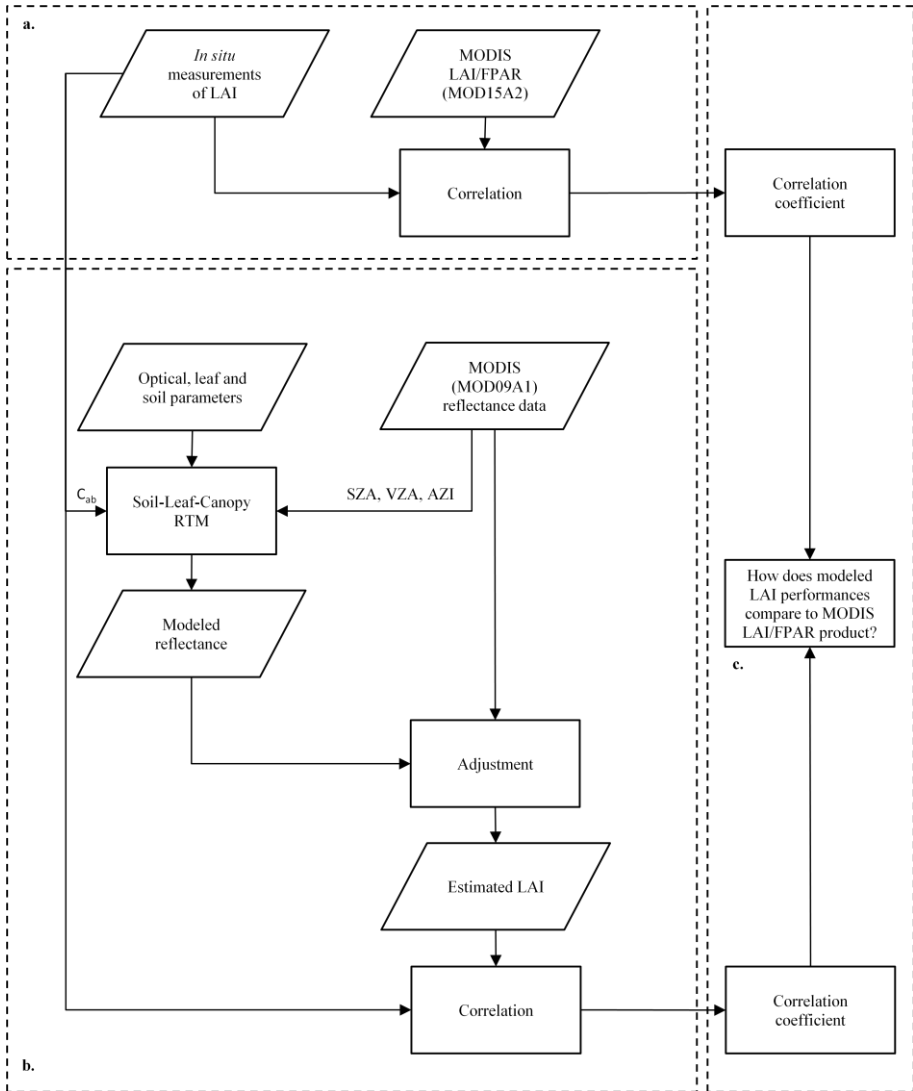


Figure 1 Methodology flowchart.

3.2. Study area

The study area is located in the south part of the city of Seville, capital and province of the autonomous community of Andalucía, Spain (Long. 5° 45' W to 6° 17' W, Lat. 36° 55' N to 37° 15') shown in Figure 2. Seville is located in the western part of Andalucía and is characterized by a Mediterranean climate, which has mild, rainy

winters and hot, dry summers. Seville has the highest average temperature of Spain with 16.7 °C. The annual rainfall in the region is highly heterogeneous with ranges from a maximum of 2,000 mm to a minimum of 170 mm (Khan et al., 2010).

Within Seville, the main production of rice is located in the marshes of the Guadalquivir River, which includes the municipalities of Isla Mayor, Puebla del Rio, Coria del Rio, Los Palacios and Villamanrique de la Condesa. Seville is the province with the highest production of rice in the entire country. In the year 2000, the production of the province reached 301,435 metric tons of rice (38% of the production of Spain). The next year the production increased in 20,000 tons, without the increase of the cultivated area. According to the producers, the increase was mainly due to good climatic conditions and a better management system of the crop. *Oryza sativa* L. var. *Puntal* is the main variety that it has been cultivated. This variety covers almost 85% of the cultivated area of the region, due to its high yield (Franquet, 2004).

The study area was chosen for two main reasons. Firstly, homogeneous cropping season and agricultural management characterize the area of production of rice in Seville. The crop season begins between the last week of May and the first of June, and ends at the end of October. This uniformity in the growing stages of the crop provided a good framework for the study, because the LAI was being monitored through the time according to the phenology of the crop. In addition, as it was mentioned before, 85% of the area is cultivated by one variety of rice, which also facilitates the monitoring of the biophysical variables of the crop. Secondly, the area of Seville has a minimum presence of clouds during the vegetative stage of the crop. By reducing the presence of cloud cover in the area, it was possible to expect better results in the study.

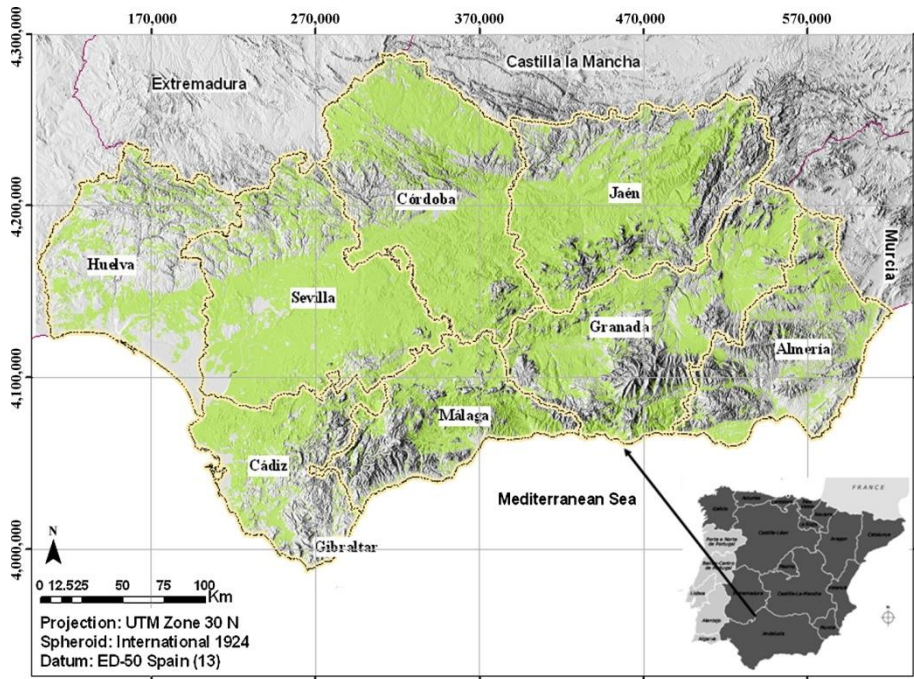


Figure 2 Location of Seville within Andalucía. Inset: location of the autonomous community of Andalucía in Spain (Khan et al., 2010).

3.3. Data used

- **MODIS products**

The data used included the hyper-temporal MODIS LAI/FPAR product (MOD15A2) 8-day composite images at 1 km of spatial resolution and the hyper-temporal MODIS surface reflectance product (MOD09A1) 8-day composite images at 500m² of spatial resolution. The images were dated from the 3rd of July to the 11th of August 2008, which corresponds to the time that the fieldwork campaign was carried out. A total number of five 8-day composite images covered the fieldwork campaign. The images were obtained from the Earth Resources Observation Service Data Center Distributed Active Archive Center (EDC DAAC) website (<https://lpdaac.usgs.gov/lpdaac/> and <https://wist.echo.nasa.gov>). The MOD15A2 and MOD09A1 products are projected on the Sinusoidal 10° grid, where the globe is divided for production and distribution purposes into 36 tiles along the east-west axis, and 18 tiles along the north-south axis, each approximately of 1200 x 1200 km (Myneni et al., 2002).

The MOD15A2 product is derived from the MODAGAGG (aggregated 1km surface reflectance), MOD12Q1 (global 1 km quarterly land cover definition) and MOD15 Ancillary data (MOD15 Ancillary data). The MODAGAGG process transforms the 250 and or 500 meter atmospherically corrected surface reflectance into a normalized 1 km form upon which all of the biophysical products are based. The LAI and FPAR products are retrieved from atmospherically corrected Bidirectional Reflectance Factors (MOD 09 Surface Reflectance Product) (Myneni et al., 2003).

The MOD09A1 product is a composite of the MOD09GHK product. MOD09A1 provides surface reflectance at 500 m resolution of seven spectral bands (620 - 670, 841 - 875, 459 - 479, 545 - 565, 1230 - 1250, 1628 - 1652 and 2105 - 2155 nm). Each pixel contains the best possible observation during an 8-day period as selected on the basis of high observation coverage, low view angle, absence of clouds or cloud shadow and aerosol loading (Vermote, 2008). The procedure to generate MOD09A1 composites first eliminates pixels with a low observational coverage, and then selects the observation with the minimum blue band values during the 8-day period (Xiao et al., 2006). The product is provided with reflectance values for bands 1 to 7, quality assessment, day of the year and solar, view and zenith angles.

- **LANDSAT 7 ETM+**

Information from LANDSAT 7 ETM+ product was also used for the study. The product provides surface reflectances at 30 m resolution of seven bands (450, 530, 630, 780, 1555, 1040, 2090 nm) and one panchromatic band of 15 m of spatial resolution (520 - 900 nm). The product gives geometric and atmospherically corrected data from the bands mentioned before. The red and NIR band of the image of the 3rd of August of 2008 were used to calculate Normalized Difference Vegetation Index (NDVI) of the plots to enhance the estimation of LAI from MODIS LAI/FPAR product.

- **Orthophotos**

A third product used in this study, were Seville's orthorectified aerial photographs (orthophotos), scale 1:20,000 at 0.50 m of spatial resolution. A mosaic was built with the orthophotos with the objective to improve the estimation of LAI from MOD15A2 together with the NDVI derived from the LANDSAT 7 ETM+ product.

3.4. Quality assessment of the MODIS LAI/FPAR product

To assess the quality of the MODIS LAI/FPAR product, correlations between values of LAI *in situ* measurements and MOD15A2 product were carried out. Both datasets required a pre-processing stage during which the data was collected and prepared for the required correlations.

3.4.1. Field data collection

For the field measurements, LAI-2000 plant canopy analyzer (LI-COR, 1992) was used. LAI was measured from above and below canopy in order to determine the canopy light interception from five angles. In addition, information about the chlorophyll content was measured using the SPAD-120. The plots were georeferenced using a handheld GPS.

Field data collection was carried out by an ITC PhD student and took place in Seville's rice production region between the 3rd of July and the 6th of August of 2008. The campaign coincided with the last vegetative stage of crop tillering (weeks 6 - 10 after sowing). A random sampling method was applied, with the sampling unit comprising a single rice field. To capture the variability within the plot, at least 6 subsamples were taken inside each sampled plot. The time was scheduled to sample each plot every week to monitor the behaviour of the LAI through time in relation with the phenology development of the crop. At the end of the campaign, 40 plots were sampled and more than 1600 subsamples were collected. The number of samples varied between plots and through time due to local conditions and difficulties that were encountered during the survey.

3.4.2. Preparation of LAI from field data

The collected data was grouped by week of collection and by plot. The grouping aimed to coincide to the periods of the 8-day composite MODIS product. Descriptive statistics were made to analyze the general behaviour of LAI. In addition, box plots graphs were made to check if the behaviour of the variable through time reflects the phenology and growing stage of the crop. Outliers were removed according to the information displayed in the box plots.

3.4.3. Preparation of LAI dataset from MOD15A2

MOD15A2 provides a product with six datasets (Table 1) in HDF-EOS format, which LAI_1km dataset was extracted for analysis.

Table 1 Science datasets specifications for MOD15A2 product (adapted from <https://lpdaac.usgs.gov/>)

Data sets	Units	Valid range	Scale factor
FPAR_1km	Percent	0 – 100	0.01
LAI_1km	m ² plant/ m ² ground	0 – 100	0.1
FPARLAI_QC	Class flag	0 – 254	na
FPARExtra_QC	Class flag	0 – 254	na

Due to the characteristics of the HDF-EOS format, the datasets are produced in a “uint8” data type, which is an unsigned 8 bit integer variable whose values may range from 0 – 255. For the case of the FPAR and LAI datasets (including standard deviation datasets), the values range from 0 – 100. Their values are stored with a scale factor that should be applied to transform them to their biophysical values for analysis according to the expression that follows (Eq. 1):

$$\mathbf{Analytical}_{pixel} = \mathbf{scale\ factor} * (\mathbf{digital}_{pixel}) \quad \mathbf{Equation\ 1}$$

Quality control (QC) datasets are added to the MOD15A2 at pixel level. The algorithm of the FPAR/LAI is executed no matter the quality of the inputs; therefore is necessary to consult the QC datasets to select reliable retrievals (the description of the codes and interpretation of the QC values can be checked in (Myneni et al., 2003).

For the quality assessment of the MODIS LAI/FPAR product, it was necessary to compare data with the same date of the fieldwork campaign. Therefore, five 8-day composite datasets of LAI were used for that purpose. The datasets were subset for the region of the rice’s production of Seville and stacked in a chronological order.

3.4.4. Disaggregation technique for MOD15A2 product

MODIS products are known by their capability to provide multi-temporal coarse resolution satellite data to monitor spatial and temporal dynamics of land cover. However, the scale of the satellite data is often not enough to explain the vegetation dynamics, especially in the case of crops. In the specific case of the MOD15A2 product, the mixed pixel problem has a big influence on the quality of the data provided as LAI or FPAR To solve this problem, a disaggregation technique focused on the estimation of the NDVI values for different land cover classes was used (Busetto et al., 2008).

This methodology is based in the linear mixing theory, which assumes that the NDVI of a mixed pixel can be calculated as the sum of mean NDVI values of the different land cover classes within the pixel, weighted by the corresponding fractional cover (Settle and Drake, 1993). The general equation, referred to the NDVI appears below (Eq. 2):

$$NDVI(i, t) = \sum_{c=1}^k (fc(i, c) \cdot NDVI_i(c, t)) + \varepsilon(i, t) \quad \text{Equation 2}$$

Where $NDVI(i, t)$ is NDVI of pixel i at time t , $fc(i, c)$ is the fractional cover of land-cover class c in pixel i , $NDVI_i(c, t)$ is the mean NDVI of a land cover class c in pixel i at time t , k is the number of land cover classes in pixel i and $\varepsilon(i, t)$ the residual error term. One of the key issues in this formulation is that it assumes linearity in the composition of the signal of the various pixel components, which is strictly valid only for the original reflectances values (Busetto et al., 2008). However, it has been demonstrated that this linearity assumption only leads to minor inaccuracies when NDVI is used instead of reflectance (Kerdiles et al., 1996). This technique derives the information about the fractional cover of each class within the low-resolution pixels as derived from the analysis of higher spatial resolution images or from ancillary data.

The general procedure used to address the mixed pixel problem is indicated in the diagram that is presented in Figure 3. For the calculation of the rice's vegetative fraction cover, four main datasets were used: Orthorectified aerial photographs for high spatial accuracy, LAI dataset from the MOD15A2 product, georeferenced plots from *in situ* measurements and a LANDSAT 7 ETM+ product of the 3rd of August of 2008 to extract fraction cover by pixel cropped. The sampled plots of the fieldwork were overlay over LAI's dataset pixel to determine number and location of the pixels suitable for the comparison.

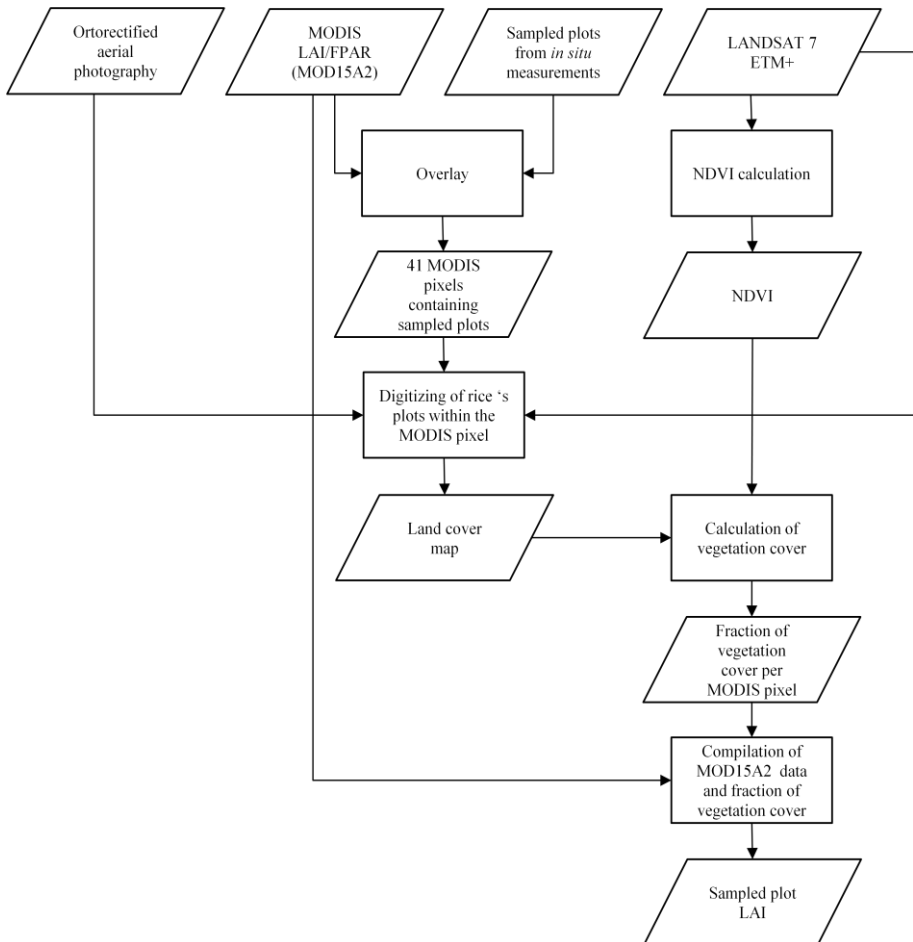


Figure 3 Overall method to solve the mixed pixel problem.

Aerial photographs were used to digitize all rice plots contained within the selected pixels from MODIS. A vegetation colour composite (4,5,2) in the LANDSAT 7 ETM+ image was used to check the areas with vegetation cover in August 2008, due to the time difference between the aerial photographs and the date that the fieldwork was carried out (Figure 4). The study area is well known by its intensive rice production; therefore, it was assumed that all the vegetative cover was rice. Figure 4 shows the contour of the MODIS pixels (yellow) overlaying the area of rice. Sampled rice plots (yellow fill) and rice plots (black contour) contained within the MODIS pixel were checked using the LANDSAT image.

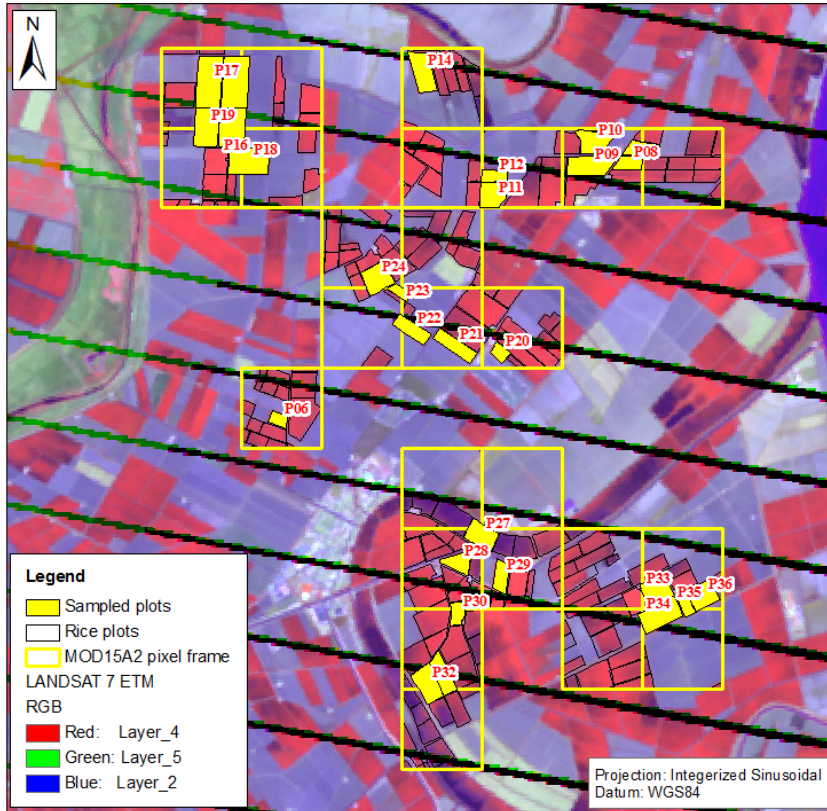


Figure 4 MOD15A2 pixels containing rice's sampled plots.

Digitalization produced a land cover map with two classes contained within 41 MODIS pixels: Rice (vegetation) and non-rice (bare soil, urban, water and roads). Within the rice class, two subclasses were defined: Sampled plots and non-sampled plots. The differentiation between sampled and non-sampled plots provided the ratio to estimate the LAI of the sampled plot. From the LANDSAT 7 ETM+ image, the NDVI was calculated with the red (630 – 690 nm) and NIR (760 – 900 nm) bands, according to the equation 3:

$$NDVI = \frac{NIR-Red}{NIR+Red} \quad \text{Equation 3}$$

The NDVI was calculated per classes (rice and non-rice) and per MODIS pixel. With the relationships between rice class and non-rice class the fraction of vegetation cover was calculated. In addition, relationships between the NDVI of sampled plots and non-sampled plots were calculated to determine the influence of the non-sampled plots over the value of the LAI from MODIS product. Finally, the

fraction of vegetation cover and the LAI dataset from MOD15A2 were compiled to calculate the value of LAI per plot per week.

3.4.5. Comparison between measured LAI values and MOD15A2 LAI values

The values of the measured LAI and the MOD15A2 LAI values were compared by a correlation, using Pearson's distribution for a level of confidence of 0.95.

3.5. Estimation of the LAI from the SLC radiative transfer model

The modelling of the LAI from the radiative transfer model required the use of information from MOD09A1 product, collected data from fieldwork and knowledge of the canopy structure of the crop.

3.5.1. Preparation of surface reflectance dataset from MOD09A1

8-day MODIS surface reflectance product (MOD09A1) was provided in HDF-EOS format, with 13 datasets (Table 2). Datasets containing information of angles (solar zenith, view zenith, relative azimuth) were used as input for the modelling of the surface reflectance. In addition, datasets of bands 1 to 7, were used as reference spectra to check the output of the RTM during the forward modelling process (Figure 1b).

3.5.2. SLC model software

An academic version of the Soil-Leaf-Canopy RTM was available for the study. The version contained the platform for modelling spectral reflectance using the Hapke soil BRDF model, PROSPECT leaf model and the 4SAIL2 model. The software of the SLC was designed as a speed-optimized Windows DLL, which allowed the efficient use of computer resources (Verhoef and Bach, 2007). The interface of the software allowed manipulating and observing how the changes in the values of the parameters influenced the reflectance response of the three models.

Table 2 Science datasets specifications for MOD09A1 product (adapted from <https://lpdaac.usgs.gov/>)

Data sets	Wavelength (nm)	Units
500m surface reflectance - Band 1	620 – 670	Reflectance
500m surface reflectance - Band 2	841 – 876	Reflectance
500m surface reflectance - Band 3	459 – 479	Reflectance
500m surface reflectance - Band 4	545 – 565	Reflectance
500m surface reflectance - Band 5	1230 – 1250	Reflectance
500m surface reflectance - Band 6	1628 – 1652	Reflectance
500m surface reflectance - Band 7	2105 - 2155	Reflectance
500 m reflectance band quality	na	Bit field
Solar zenith angle	na	Degree
View zenith angle	na	Degree
Relative azimuth angle	na	Degree
500 m state flags	na	Bit field
Day of year	na	Julian day

3.5.3. Look-up table inversion

For the estimation of the LAI, a modified look-up table (LUT) approach used by Darvishzadeh et al. (2008a) was chosen. The authors used this approach for the inversion of a RTM to estimate LAI in heterogeneous grasslands. This approach was considered for this study due to the simplicity of the method, the data collected during the field campaign and the characteristics of the interface of SLC. However, changes were made to the method in order to make it suitable for the SLC estimation of LAI.

The LUT approach required a forward modelling of the surface's reflectance using parameters based on the physical structure of the canopy, spectral properties of the canopy and its background, and biophysical variables of the crop. Table 3 presents a summary of the parameters used for the process. Modelled values of spectral reflectance from the RTM were adjusted using values of the MOD09A1 product pixels. The software of SLC provided a tool to adjust manually the estimated spectral reflectance to a given reflectance. Due to the nature of the method, the adjustment of the spectral reflectances was made between NIR bands (Meroni et al., 2004). After the spectral reflectance was adjusted to the reflectance values of MOD09A1, the value of LAI retrieved for that set of parameters and adjustments

was annotated (. For each MOD09A1 pixel that contained a sampled plot, the retrieval of the LAI was made.

Table 3 Soil, leaf and canopy parameters used for the forward modelling of the surface reflectance of rice.

Model	Parameter	Value
Soil	Soil code (single scattering albedo)	75
	Soil Hapke b	0.84
	Soil Hapke c	0.68
	Soil Hapke B_0	0.30
	Soil Hapke h	0.23
	SM%	5
Leaf (PROSPECT)	N green leaves	1.5
	C_{ab} green leaves	55
	C_w green leaves	0.02
	C_{dm} green leaves	0.005
	C_s green leaves	0.00
	N brown leaves	--- *
	C_{ab} brown leaves	--- *
	C_w brown leaves	--- *
	C_{dm} brown leaves	--- *
C_s brown leaves	--- *	
Canopy (4SAIL2)	LAI	1.0 – 8.0
	LIDF a	- 0.5
	LIDF b	- 0.5
	D	0.80
	Hotspot size	Varied with LAI (0.5/LAI)
	f_B	0
	C_v	100
	zeta	na
	sza	Varies with MODIS pixel
	vza	Varies with MODIS pixel
	raa	Varies with MODIS pixel

* During the vegetative stage of the crop, is assumed that the canopy consists only of green leaves.

The parameters of Hapke's model described in Table 3 are five: b and c which are the parameters of the scattering phase function described by Pinty et al. (1989). B_0 and h describe the magnitude and half width of the hot spot peak, respectively. SM % indicates the percentage of soil moisture. These parameters were set equal to the default values obtained for a ploughed soil (Pinty et al., 1989).

Leaf parameters from PROSPECT are five, each one described twice for green and brown leaves. N describes the leaf structure; C_{ab} , the content of the chlorophyll $a + b$ ($\mu\text{g cm}^{-2}$); C_w , as the equivalent water thickness (cm); and C_{dm} , the dry matter content (g cm^{-2}) (Jacquemoud et al., 2009). The value of N was selected according to the one suggested for various crops by Houborg, et al. (2007) cited by Darvishzadeh (2008a). Chlorophyll content (C_{ab}) was measured on the field during the campaign using a SPAD-120.

Parameters for 4SAIL2 are eleven, describing biophysical and optical characteristics of the canopy. LAI refers to Leaf Area Index; $LIDF_a$ and $LIDF_b$ describe the leaf inclination distribution function; the parameter a controls the average leaf slope and the parameter b controls the distribution's bimodality. D , describes the layer dissociation factor; f_B , the fraction brown leaf area; C_v the vertical crown cover percentage and ζ the tree shape factor (which was not used for this modelling). S_{za} , v_{za} and r_{aa} describe the sun zenith angle, vertical zenith angle and relative azimuth angle, respectively. Values of the LIDF parameters were selected according to the type of the crop and suggestions by Verhoef (2010). The soil code chosen (75) belonged to the single scattering albedo of a soil under a thin layer of water, which corresponds to the growing characteristics of rice. Values of sun zenith angle, vertical zenith angle and azimuth angle were selected according to the values given by the MOD09A1 product. Due to the lack of other leaf and canopy parameters for rice, values of maize used by Verhoef and Bach (2007) were kept for the modelling. Maize was selected due to its structural and physiological similarities with rice.

3.5.4. Comparison between measured values and estimated LAI from SLC

Modelled values of the measured LAI and the SLC's LAI values were compared by a correlation, using Pearson's distribution for a level of confidence of 0.95.

4. Results

4.1. Quality assessment of the MODIS LAI/FPAR product

4.1.1. Correction of LAI measurements from field

After the analysis of the field data, it was detected that daily values of LAI were a function of the hour of the day. A trend of lower values of LAI was detected when the hour of collection was around 15:30 hours (Figure 5).

According to the manual of the LAI-2000, underestimation of LAI is due to the effect of direct sunlight over the foliage. This underestimation is common during days with clear skies or when the sun is not close to the horizon. It has been reported that the underestimation of LAI due to direct sunlight ranges from 10% to 50%, especially in canopies with large gaps. For such cases it is recommended that if it is not possible to repeat the measurements, an interpolation over time could work well (LI-COR, 1992).

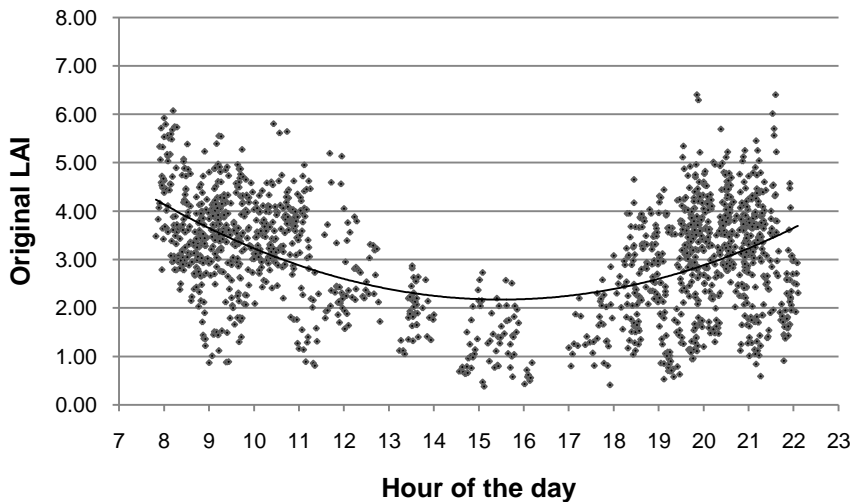


Figure 5 Behaviour of measured values as a function of time of the day.

Following the recommendation, an iterative method of visual transformation was carried out to adjust the values. Values between 10:00 and 21:00 hours were adjusted, considering the variation between them and the data collected close to sunrise or sunset. A function explaining the behaviour of values contained within the range was defined (Eq. 4). The function provided information about the trend of the

values and their variation. This information was useful for the transformation, since the new values must contain the same variation as the one showed at the beginning. Once the function was defined, values of adjustment were estimated by mean of iterations. The adjustment was defined averaging values of LAI for the measurements made close to 10:00 and 21:00. This average provided the information about the pattern that the original values should follow if the collection of data were not carried out under direct sunlit conditions. The final equation with the adjustment value for the correction of the data is present as follows:

$$CLAI_{10-21} = \frac{OLAI_{10-21} * k}{18.92 - 2.222 H + 0.07156 H^2} \quad \text{Equation 4}$$

Where $CLAI_{10-21}$ is the corrected LAI for the measurements made between 10:00 and 21:00. $OLAI_{10-21}$ is the original value of LAI measured in field between 10:00 and 21:00, and k is the adjusted coefficient. H represents the hour of the day (decimals) where the measurement was taken. The results of the correction with the general trend of the data are shown in Figure 6 .

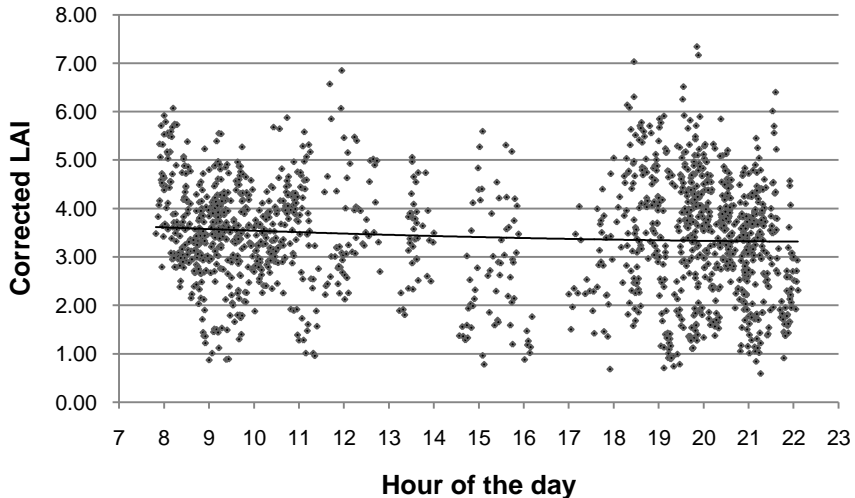


Figure 6 Corrected LAI values after the transformation.

Figure 6 shows the trend of the corrected values of LAI. The underestimation detected between 10:00 and 21:00 was removed and now a trend with values non-dependent of the hour of the day can be observed. Values beyond the range were left with their original values. In addition, is possible to observe that the variation of the corrected values increased following the pattern of the other values outside the

range. Figure 7 shows the comparison between the corrected values and the original values of the LAI. Trend lines were added to show that the adjustments made increased the values of the LAI, correcting the original underestimation.

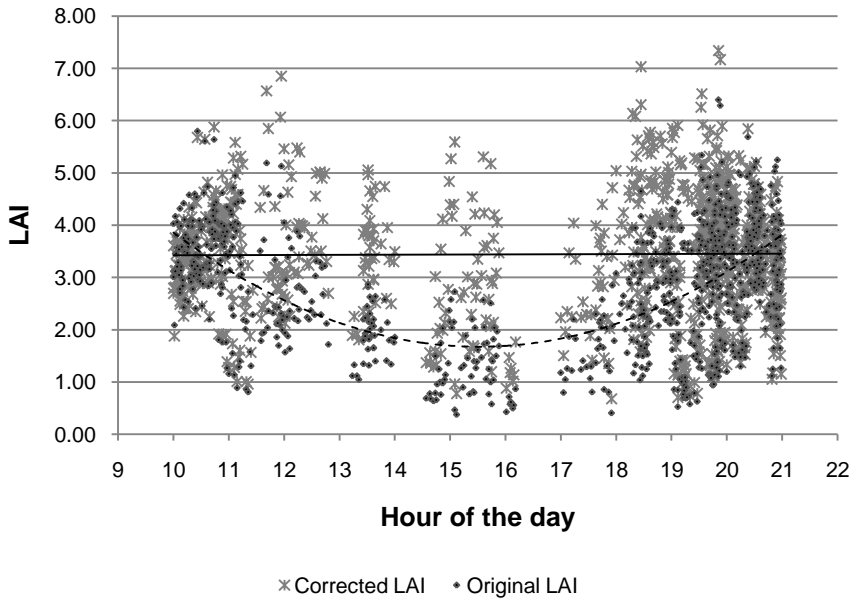


Figure 7 Comparison between corrected values and original values with their respective trend lines.

After the correction of the dataset, a correlation analysis between observed and corrected data was carried out to verify the behaviour of the new dataset. Figure 8 shows the behaviour of the scattered plot which provided a correlation coefficient of $R = 0.8746$. In the figure is possible to observe two strong patterns of behaviour between corrected and original values. The bottom pattern shows the values that were not changed (outside the range 10 – 21 hours); meanwhile the upper pattern shows the values that were corrected giving higher LAI values.

A histogram with the corrected values of LAI was used to observe the behaviour of the dataset with the new values (Figure 9). The pattern showed a normal distribution, which was the expected pattern after the transformation.

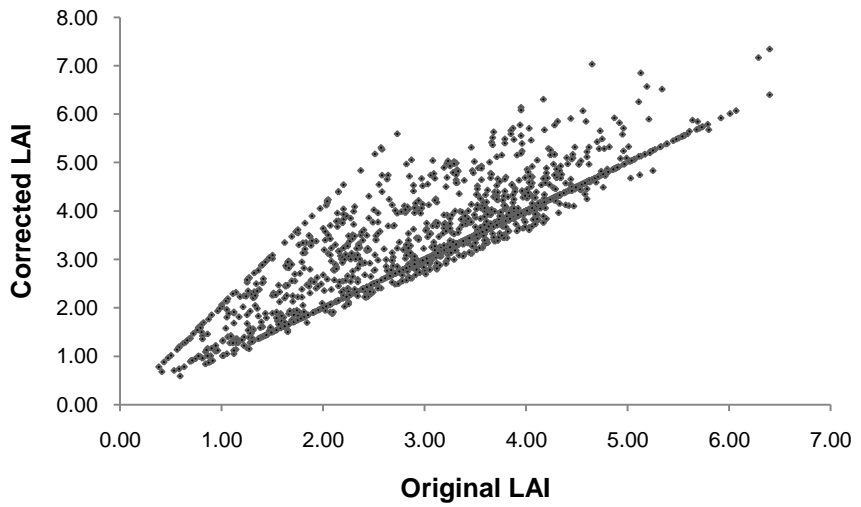


Figure 8 Comparison between original and corrected LAI.

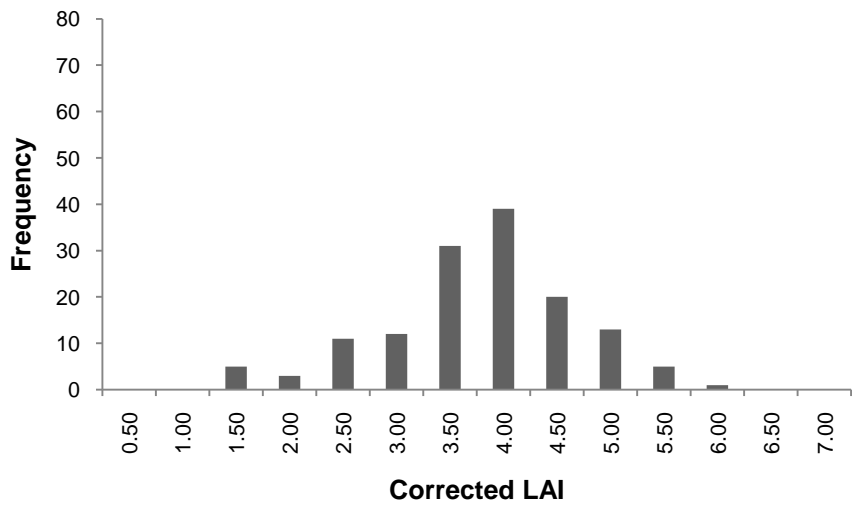


Figure 9 Histogram of the corrected values of LAI measured in the field (per week).

4.1.2. Comparison between LAI values from the field and MOD15A2

With the disaggregation technique based on NDVI, LAI values from the MODIS product were estimated for the sampled plots. Due to the nature of the product (8-day composite), weekly values of LAI were estimated. A histogram was used to observe the behaviour of the variable, as is shown in Figure 10. The histogram showed a positive skewness, indicating that most of the values were located between the range of 0.50 and 2.00.

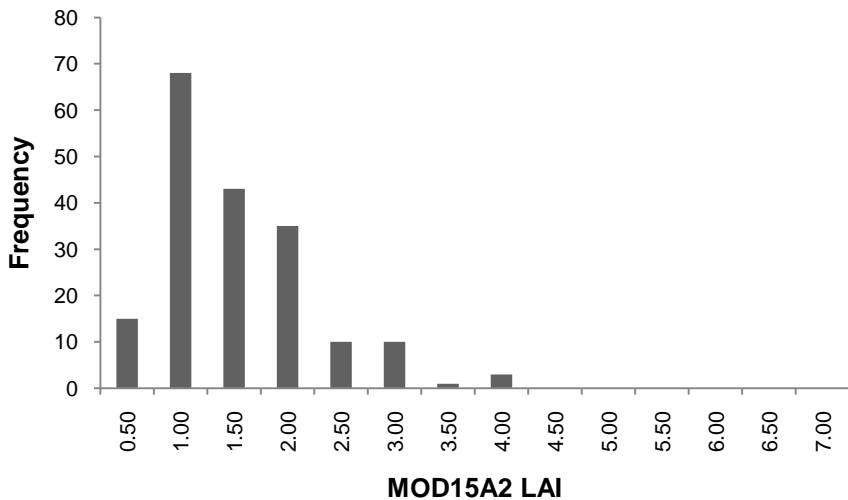


Figure 10 Histogram of the MOD15A2 product.

A correlation between corrected values of LAI versus MOD15A2 values of LAI was carried out to assess the values from the MODIS product. The dataset for the correlation consisted in 129 pairs of LAI values grouped by week (Appendix A). The Pearson's correlation coefficient was calculated, giving a value of $R = 0.447$. Figure 11 shows the scatter plot of the compared datasets. The line symbolizes the pattern that the values should follow if a perfect correlation exists (1:1).

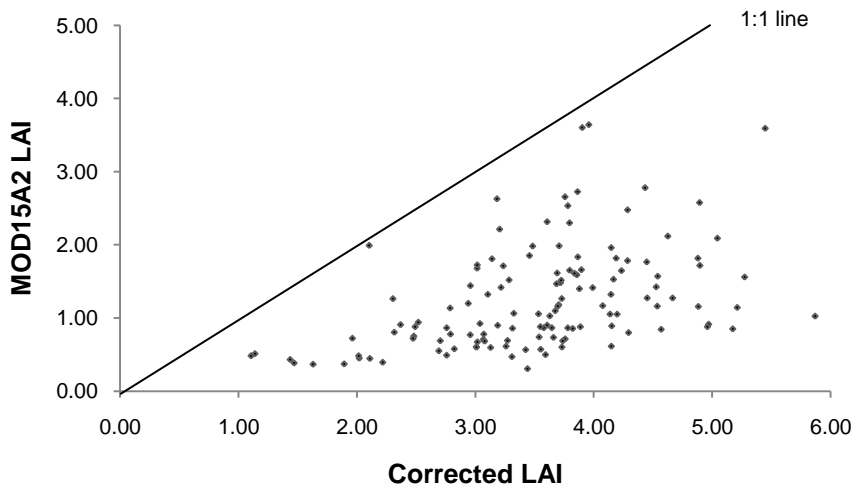


Figure 11 Comparison between LAI values from the field and MOD15A2

LAI estimated from MODIS15A2 shows lower values than LAI measured in the field. The scatter plot shows that MOD15A2 underestimates values of LAI compared to values measured in the field. In addition, the scatter plot demonstrates that the range of values produced by MOD15A2 is smaller than the values measured in the field.

Correlations between both datasets were calculated per week, in order to observe the behaviour of the data without the effect of time. Figure 12 and Figure 13 show the behaviour of the sixth and ninth week after sowing, respectively. In Figure 12, the pattern of lower LAI values from MOD15A2 compare to measured values, repeats. In this case, it was not possible to identify the trend that was obvious in Figure 11, which covered the vegetative stage. Figure 13 shows the underestimation of LAI from MOD15A2, but in this case, a small change in the lower values of MODIS LAI is evident compared to week 6. Contrary to Figure 12, the range of LAI values from MOD15A2 is higher.

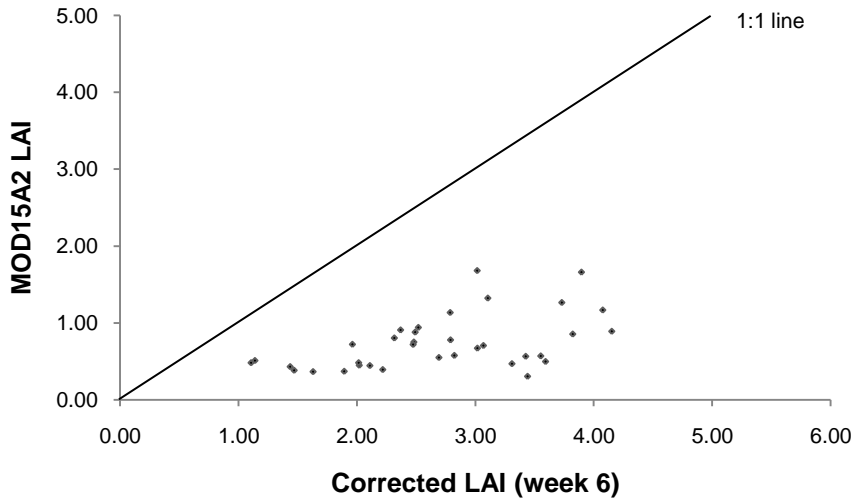


Figure 12 Scatter plot of the correlation between corrected LAI from the field and MOD15A2 LAI for the first week of the fieldwork campaign (6th week after sowing).

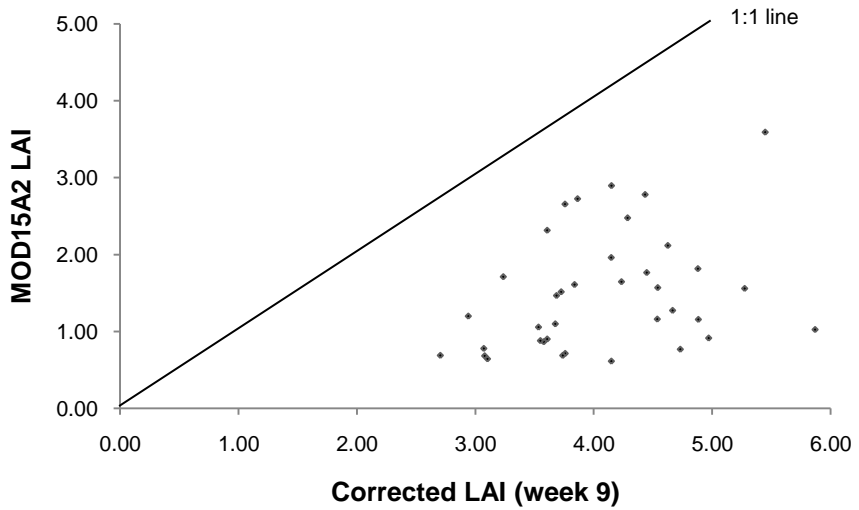


Figure 13 Scatter plot of the correlation between corrected LAI from the field and MOD15A2 LAI for the 4th week of the fieldwork campaign (9th week after sowing).

4.2. Estimation of LAI from SLC and quality assessment

Values of LAI were estimated from the inversion of the SLC model. According to the temporal level of the study, values of LAI per week for each measured plot on field were calculated. Following the procedure for the evaluation of the LAI in 4.1, a histogram with all the estimated values of LAI was made to observe the behaviour of the variable as is presented in Figure 14. The histogram showed most of values located below 4.00 with a positive skewness.

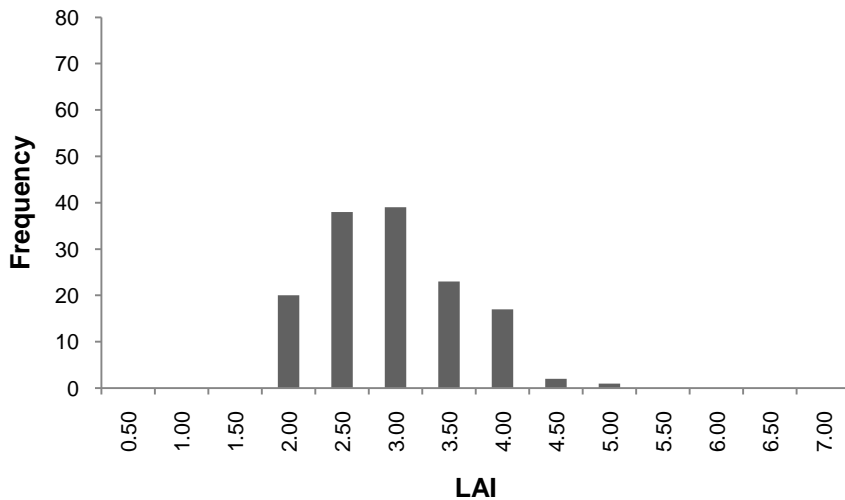


Figure 14 Histogram of the values of LAI estimated with SLC.

Comparisons between estimated values from SLC and corrected values from the field showed a Person's correlation coefficient of $R = 0.497$. The dataset used for the comparison consisted of 140 pairs of LAI values grouped by plot and week (Appendix B). Figure 15 shows the comparison between estimated and corrected values. The line shows a 1:1 line that values should follow if a perfect correlation exists. LAI estimated from SLC shows lower values than the LAI measured in the field. The scatter plot also demonstrates that SLC underestimates observed values of LAI, when values are higher. The range of values of the estimated LAI is smaller than the corrected LAI. Following the same analysis that was done for the MODIS product, correlation between estimated values of LAI from SLC and measured values per week were carried out. This analysis aimed to observe the behaviour of the variable without the influence of time.

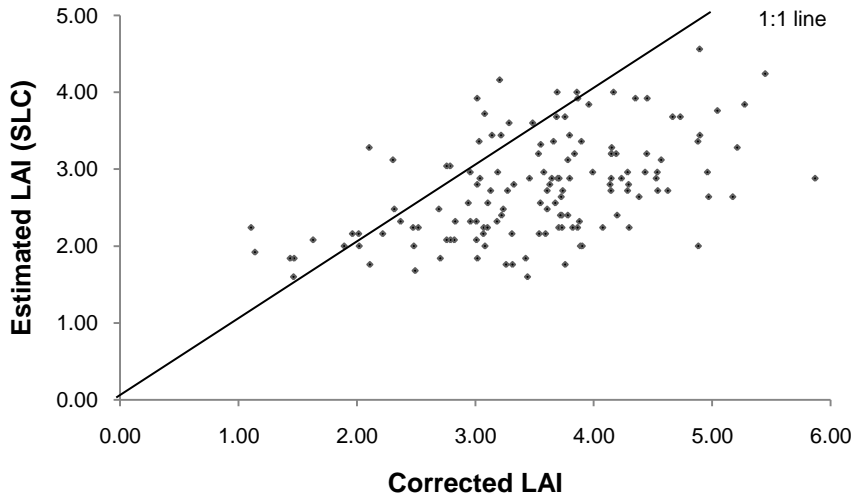


Figure 15 Comparison between LAI from field and from SLC.

In the same way that the analysis for the MODIS LAI/FPAR product was made, comparisons for the week 6 and week 9 were carried out between SLC values and *in situ* measurements. Figure 16 shows the correlation for the week 6, where there SLC shows a slightly underestimation of LAI values compared to field data. More than 60% of the data is located below the 1:1 line, which indicates a trend to underestimate LAI when the values measured in the field increase.

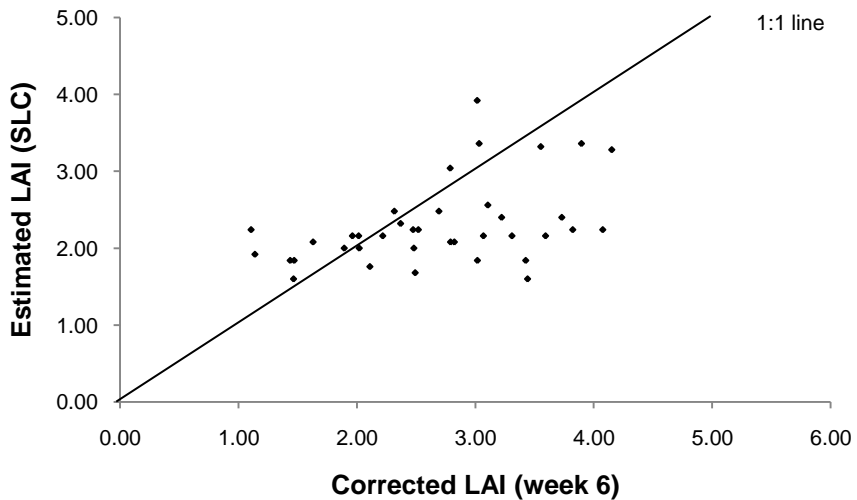


Figure 16 Scatter plot of the correlation between LAI from the field and from SLC for the first week of the fieldwork campaign (6th week after sowing).

Figure 17 shows the behaviour of the values during the 9th week after sowing. The scatter plot shows that higher values of estimated LAI increase the underestimation compared to *in situ* measurements. The pattern detected in the previous figure is confirmed, locating almost 100% of the data below the 1:1 line.

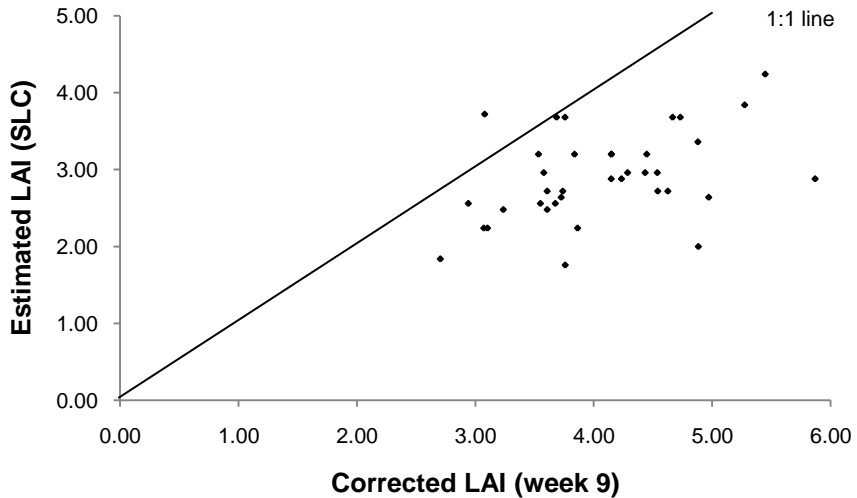


Figure 17 Scatter plot of the correlation between LAI from the field and from SLC for the 4th week of the fieldwork campaign (9th week after sowing).

4.3. Comparison between estimated LAI from SLC and MOD15A2 LAI

Estimated values from SLC and MOD15A2 values were compared using a scatter plot as is shown in Figure 18. Pearson’s correlation coefficient was calculated, obtaining a value of $R = 0.546$. In this case, MOD15A2 product shows lower values compared to estimated LAI from SLC. The trend showed on the plot corresponds to the behaviour observed in the histograms of both datasets, with values of MOD15A2 with a higher positive skewness compared to SLC values.

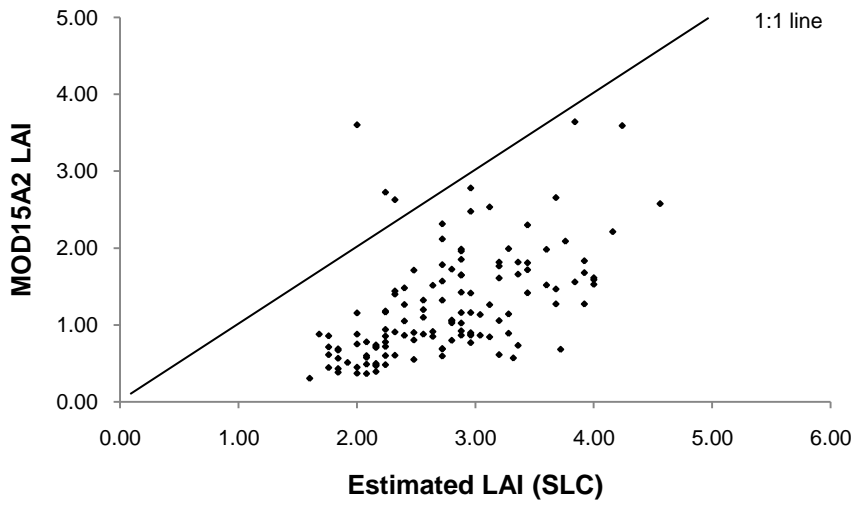


Figure 18 Scatter plot of the estimated values of LAI and MOD15A2 LAI values.

5. Discussion

5.1. Quality assessment of the MODIS LAI/FPAR product

Values of LAI from 8-day composite MODIS LAI/FPAR product (MOD15A2) differed with the values of LAI collected in the field. The MODIS product could explain only 45% of the variation of field measurements of rice. There was a generalized trend of the product to underestimate values of LAI compared to field measurements (Figure 11). According to Fensholt et al. (2004), underestimations of LAI by MODIS are consequence of coarse resolution data, which increases that amount of radiation reflected from the background within a pixel. The magnitude of the underestimation of LAI increases as vegetation heterogeneity increases (Tian et al., 2002). The site of rice's production in Seville is well known by its homogeneity; therefore, the underestimation due to the heterogeneity of the vegetation can be discarded. However, the coarse resolution data should be taken in account, moreover if the background of the coarse pixel includes water. In addition, it is important to consider that the coarse resolution of the data is also affected by the temporal dynamics of the crop. During the transplanting stage of the rice, flooded soils are required and after 60 days the canopy cover most of the background (Xiao et al., 2005). This indicates that within 2 months, the environment of the crop changes in marked contrasts, which affects the performance of the algorithm for the retrievals of the LAI. The behaviour of the values of LAI from Figure 12 and Figure 13 could explain these changes and the problems of the algorithm to retrieve the values of LAI. Values of week 6 showed less variability compared to week 9, which can be explained by the influence of the seasonal dynamics and the effect of the growing canopy covering the background. In early stages, the surface is a mixture of crop greenness, water and mud, meanwhile close to the 60th day after sowing (9 – 10 week) the canopy covers most of the soil, providing a more uniform surface and thus better conditions for the estimation of the LAI.

On the other hand, Hill et al. (2006) observed that the algorithm of the MODIS product could perform well only if the six biome land cover classification of the product allocates the correct class according to reality. The region that contains the rice zone in Seville is known to be an area of agricultural production. However, dynamics in agronomic systems could influence changes in land use, which could affect the land cover classification and thus the correct allocation of the biome. 2008 reported a decreased in yielded rice in Seville, due to the increase of growth of other crops with different physiological and phenological behaviour. These issues are the

ones that should be considered to understand the underestimation of the LAI from MODIS.

5.2. Estimation of LAI from SLC and quality assessment

Values of LAI from SLC model could explain 50% of the variation of the values of LAI measured in the field. Although the correlation coefficient did not differ much to the one calculated for MOD15A2, SLC retrieved less underestimated values (Figure 15). The 1:1 line drawn in the figure shows at least 30% of the values located in the upper bound, which indicated better performance compared to the MOD15A2 product. However, when the values of the estimated LAI were compared with measured LAI values per week, it was noticed that SLC underestimated LAI with higher values of LAI from field (week 9).

One cause of the underestimation could be the use of many parameters derived from other types of vegetation. However, without a sensitivity analysis, the cause of the underestimation only can only be considered nothing more than a hypothesis. Nevertheless is important to consider that too many parameters for a specific type of vegetation in specific conditions could result in a model impossible to generalize (Qin et al., 2008).

Another cause of the underestimation of higher values could be addressed to the method used for the inversion. According to Meroni et al., (2004), at least three bands should be used initially for the inversion of a model (red, near-infrared, and shortwave infrared). However, later on it was considered that the nature of the method and the slowness of it, would allow using only one band of MOD09A1 for the inversion. Following the recommendation of Wang and Huang (2009), NIR (841 – 875 nm) band of MOD09A1 was selected due to its strong relation with LAI retrievals. The problem of retrieving values of LAI based on NIR was similar to the one between LAI and NDVI (saturation of NDVI for LAI higher values). This effect could explain the influence of the retrievals on the underestimation of LAI for higher values of field measurements. Many authors (Meroni et al., 2004; Darvishzadeh et al., 2008a; Wang and Huang, 2009) recommend the use of various bands to perform inversions with more precision. More bands require more computational procedures and combinations of parameters to perform good retrievals of biophysical variables.

6. Conclusions

Correlations carried out between MODIS LAI/FPAR product (MOD15A2) and *in situ* measurements of LAI for rice showed a Person's correlation coefficient of 0.447. This indicates that less than 45% of the variation of *in situ* measurements was explained by MODIS LAI/FPAR product. According to stage of the crop where the study was carried out (vegetative stage), an increasing trend of LAI values was expected. MODIS LAI/FPAR product was able to detect this increasing trend but with a marked underestimation of the biophysical variable compared to field measurements. The differences between the values of LAI could be attributed to the coarse resolution of the MODIS product; effect of the water background on the spectral reflectances that the algorithm requires as input data, and the criteria of which the algorithm retrieves information according to a predefined biome.

Estimated values of LAI from Soil-Leaf-Canopy showed a Pearson's correlation coefficient of 0.497, which indicates that the model explains less than 50% of the variation of *in situ* measurements. It is important to mention that values of SLC showed less underestimation of LAI values compared to the MODIS LAI/FPAR product. The differences between the estimated values and *in situ* measurements could be attributed to the lack of precise information for the input parameters required by the model and the criteria used for the adjustment of the modelled spectral reflectances.

LAI values estimate from SLC improved 10% the performance of the MODIS LAI/FPAR product. The main difference between the performance of the model and MODIS was the underestimation of LAI. Values of LAI from SLC showed stronger correlations with *in situ* measurements, estimating values close the 1:1 line assumed for a perfect correlation. Despite the low improvement in the performance of the MODIS LAI/FPAR product, SLC showed a high potential for the retrieval of biophysical variables.

7. Limitations and recommendations

7.1. Limitations

- Due to the historical information of the zone, uniformity in the agricultural management of the crop was assumed, indicating that differences between sowing dates, fertilization and irrigation systems were not considered. In addition, optimal growth conditions of the rice were considered, obviating the influence of external agents in the development of the crop. However, information about fluctuations in rice production indicates that 2008 was an unusual year with remarkable changes in the land use and cultivation patterns.
- NDVI values from LANDSAT 7 ETM+ were considered for the disaggregation method to avoid the mixed pixel problem despite of the presence of stripes (a very well known problem of LANDSAT product).
- The 8-day composite MOD09A1 product was considered most appropriate for the inversion and estimation of LAI, compared to other MODIS products with shorter temporal resolutions (daily).
- Due to the lack of information of the spectral signatures of rice, the spectral reflectance of the MOD09A1 product was considered ground truth for the adjustment of spectral reflectance values modelled by the SLC.
- For the modelling of spectral reflectance from SLC, parameters from ploughed soil were considered for the Hapke model, which differ from the soil for rice cultivation. The effect of this parameter in the spectral reflectance could affect notoriously the performance of the inversion.
- A manual procedure of adjustment of spectral reflectances was carried out due to the lack of an inversion module for the SLC model.

7.2. Recommendations

- During fieldwork campaigns, measurements of LAI using LAI-2000 should be carried out during sunrise or sunset to avoid the sunlit from the canopy that affects the readings of the equipment.

- The inversion of the SLC model requires further refinement. In order to perform an inversion of a radiative transfer model, measurements of spectral reflectances from the field (with the aid of a spectroradiometer) are strongly recommended. In the particular case of rice, spectral measurements of muddy soil, flooded soil and top of canopy could improve considerably the inversion. If it is not possible to obtain the spectral reflectance from field measurements, downscaling the information of SLC to MODIS spatial resolution (mixed pixel) can improve the model's performance.
- Perform retrievals of biophysical variables using more than one band.
- Soil-Leaf-Canopy model requires a high number of parameters to perform the modelling of spectral reflectances (forward) or biophysical variables (inversion). However, a greater number of parameters leads to highly specific complex models. Balance between simplicity and an accurate representation of reality must be taken into account when modelling.

8. References

- Bacour, C., Jacquemoud, S., Tourbier, Y., Dechambre, M. and Frangi, J. P. 2002. 'Design and analysis of numerical experiments to compare four canopy reflectance models'. *Remote Sensing of Environment*, vol. 79, no. 1, pp. 72-83.
- Busetto, L., Meroni, M. and Colombo, R. 2008. 'Combining medium and coarse spatial resolution satellite data to improve the estimation of sub-pixel NDVI time series'. *Remote Sensing of Environment*, vol. 112, no. 1, pp. 118-131.
- Clevers, J. G. P. W. and van Leeuwen, H. J. C. 1996. 'Combined use of optical and microwave remote sensing data for crop growth monitoring'. *Remote Sensing of Environment*, vol. 56, no. 1, pp. 42-51.
- Colombo, R., Bellingeri, D., Fasolini, D. and Marino, C. M. 2003. 'Retrieval of leaf area index in different vegetation types using high resolution satellite data'. *Remote Sensing of Environment*, vol. 86, no. 1, pp. 120-131.
- Combal, B., Baret, F., Weiss, M., Trubuil, A., Macé, D., Pragnère, A., Myneni, R., Knyazikhin, Y. and Wang, L. 2003. 'Retrieval of canopy biophysical variables from bidirectional reflectance: Using prior information to solve the ill-posed inverse problem'. *Remote Sensing of Environment*, vol. 84, no. 1, pp. 1-15.
- Darvishzadeh, R., Skidmore, A., Schlerf, M. and Atzberger, C. 2008a. 'Inversion of a radiative transfer model for estimating vegetation LAI and chlorophyll in a heterogeneous grassland'. *Remote Sensing of Environment*, vol. 112, no. 5, pp. 2592-2604.
- Darvishzadeh, R., Skidmore, A., Schlerf, M., Atzberger, C., Corsi, F. and Cho, M. 2008b. 'LAI and chlorophyll estimation for a heterogeneous grassland using hyperspectral measurements'. *ISPRS Journal of Photogrammetry and Remote Sensing*, vol. 63, no. 4, pp. 409-426.
- Fensholt, R., Sandholt, I. and Rasmussen, M. S. 2004. 'Evaluation of MODIS LAI, fAPAR and the relation between fAPAR and NDVI in a semi-arid environment using in situ measurements'. *Remote Sensing of Environment*, vol. 91, no. 3-4, pp. 490-507.
- Feret, J.-B., François, C., Asner, G. P., Gitelson, A. A., Martin, R. E., Bidet, L. P. R., Ustin, S. L., le Maire, G. and Jacquemoud, S. 2008. 'PROSPECT-4 and 5: Advances in the leaf optical properties model separating photosynthetic pigments'. *Remote Sensing of Environment*, vol. 112, no. 6, pp. 3030-3043.
- Franquet, J. M. 2004. Variedades y mejoras del arroz: *Oryza sativa*, L. In: BERNIS, J. M. F. (ed.).
- Gobron, N., Pinty, B. and Verstraete, M. M. 1997. 'Theoretical limits to the estimation of the leaf area index on the basis of visible and near-infrared remote sensing data'. *Geoscience and Remote Sensing, IEEE Transactions on*, vol. 35, no. 6, pp. 1438-1445.
- Haboudane, D., Miller, J. R., Pattey, E., Zarco-Tejada, P. J. and Strachan, I. B. 2004. 'Hyperspectral vegetation indices and novel algorithms for predicting green

- LAI of crop canopies: Modeling and validation in the context of precision agriculture'. *Remote Sensing of Environment*, vol. 90, no. 3, pp. 337-352.
- Hapke, B. W. 1981. 'Bi-directional reflectance spectroscopy 1. Theory'. *Journal of Geophysical Research*, vol. 86, no., pp. 3039-3054.
- Hill, M. J., Senarath, U., Lee, A., Zeppel, M., Nightingale, J. M., Williams, R. J. and McVicar, T. R. 2006. 'Assessment of the MODIS LAI product for Australian ecosystems'. *Remote Sensing of Environment*, vol. 101, no. 4, pp. 495-518.
- Houborg, R. and Boegh, E. 2008. 'Mapping leaf chlorophyll and leaf area index using inverse and forward canopy reflectance modeling and SPOT reflectance data'. *Remote Sensing of Environment*, vol. 112, no. 1, pp. 186-202.
- Houborg, R., Soegaard, H. and Boegh, E. 2007. 'Combining vegetation index and model inversion methods for the extraction of key vegetation biophysical parameters using Terra and Aqua MODIS reflectance data'. *Remote Sensing of Environment*, vol. 106, no. 1, pp. 39-58.
- Huang, D., Knyazikhin, Y., Dickinson, R. E., Rautiainen, M., Stenberg, P., Disney, M., Lewis, P., Cescatti, A., Tian, Y., Verhoef, W., Martonchik, J. V. and Myneni, R. B. 2007. 'Canopy spectral invariants for remote sensing and model applications'. *Remote Sensing of Environment*, vol. 106, no. 1, pp. 106-122.
- Jacquemoud, S. and Baret, F. 1990. 'PROSPECT: A model of leaf optical properties spectra'. *Remote Sensing of Environment*, vol. 34, no. 2, pp. 75-91.
- Jacquemoud, S., Verhoef, W., Baret, F., Bacour, C., Zarco-Tejada, P. J., Asner, G. P., François, C. and Ustin, S. L. 2009. 'PROSPECT + SAIL models: A review of use for vegetation characterization'. *Remote Sensing of Environment*, vol. 113, no. Supplement 1, pp. S56-S66.
- Jinsong, C., Hui, L., Aixia, L., Yun, S. and Limin, Y. 2007. 'A semi-empirical backscattering model for estimation of leaf area index (LAI) of rice in southern China'. *2007 IEEE International Geoscience and Remote Sensing Symposium*, vol., no., pp. 3667-3680.
- Kerdiles, H., Grondona, M., Rodriguez, R. and Seguin, B. 1996. 'Frost mapping using NOAA AVHRR data in the Pampean region, Argentina'. *Agricultural and Forest Meteorology*, vol. 79, no. 3, pp. 157-182.
- Khan, M. R., de Bie, C. A. J. M., van Keulen, H., Smaling, E. M. A. and Real, R. 2010. 'Disaggregating and mapping crop statistics using hypertemporal remote sensing'. *International Journal of Applied Earth Observation and Geoinformation*, vol. 12, no. 1, pp. 36-46.
- Knyazikhin, Y., Glassy, J., Privette, J. L., Tian, Y., Lotsch, A., Zhang, Y., Wang, J. D., Morisette, J. T., Votava, P., Myneni, R., Nemani, R. R. and Running, S. W. 1999. MODIS Leaf Area Index (LAI) and Fraction of Photosynthetically Active Radiation Absorbed by Vegetation (FPAR) Product (MOD15) Algorithm Theoretical Basis. Available: <http://eosps0.gsfc.nasa.gov/atbd/modistables.html> [Accessed August, 2009].
- Knyazikhin, Y., Martonchik, J. V., Myneni, R. B., Diner, D. J. and Running, S. W. 1998. 'Synergistic algorithm for estimating vegetation canopy leaf area

- index and fraction of absorbed photosynthetically active radiation from MODIS and MISR data'. *J. Geophys. Res.*, vol. 103, no., pp.
- Kobayashi, H., Suzuki, R. and Kobayashi, S. 2007. 'Reflectance seasonality and its relation to the canopy leaf area index in an eastern Siberian larch forest: Multi-satellite data and radiative transfer analyses'. *Remote Sensing of Environment*, vol. 106, no. 2, pp. 238-252.
- Koetz, B., Baret, F., Poilvé, H. and Hill, J. 2005. 'Use of coupled canopy structure dynamic and radiative transfer models to estimate biophysical canopy characteristics'. *Remote Sensing of Environment*, vol. 95, no. 1, pp. 115-124.
- LI-COR 1992. LAI-2000 Plant Canopy Analyzer Instruction/Operating Manual. Lincoln, NE, USA: Licor Inc.
- Liang, S. 2004. *Quantitative remote sensing of land surfaces*, New York, Hoboboken, NJ : Wiley-Interscience.
- Meroni, M., Colombo, R. and Panigada, C. 2004. 'Inversion of a radiative transfer model with hyperspectral observations for LAI mapping in poplar plantations'. *Remote Sensing of Environment*, vol. 92, no. 2, pp. 195-206.
- Myneni, R. B., Hoffman, S., Knyazikhin, Y., Privette, J. L., Glassy, J., Tian, Y., Wang, Y., Song, X., Zhang, Y., Smith, G. R., Lotsch, A., Friedl, M., Morisette, J. T., Votava, P., Nemani, R. R. and Running, S. W. 2002. 'Global products of vegetation leaf area and fraction absorbed PAR from year one of MODIS data'. *Remote Sensing of Environment*, vol. 83, no. 1-2, pp. 214-231.
- Myneni, R. B., Knyazikhin, Y., Glassy, J., Votava, P. and Shabanov, N. V. 2003. User's Guide FPAR, LAI (ESDT: MOD15A2) 8-day Composite NASA MODIS Land Algorithm.
- Pinty, B., Verstraete, M. M. and Dickinson, R. E. 1989. 'A physical model for predicting bidirectional reflectances over bare soil'. *Remote Sensing of Environment*, vol. 27, no. 3, pp. 273-288.
- Qin, J., Liang, S. L., Li, X. W. and Wang, J. D. 2008. 'Development of the adjoint model of a canopy radiative transfer model for sensitivity study and inversion of leaf area index'. *Ieee Transactions on Geoscience and Remote Sensing*, vol. 46, no. 7, pp. 2028-2037.
- Ross, J. K. 1981. *The radiation regime and architecture of plant stands*, Norwell, MA, Dr. W. Junk, Publishers.
- Settle, J. J. and Drake, N. A. 1993. 'Linear mixing and the estimation of ground cover proportions'. *International Journal of Remote Sensing*, vol. 14, no. 6, pp. 1159 - 1177.
- Stroppiana, D., Boschetti, M., Confalonieri, R., Bocchi, S. and Brivio, P. A. 2006. 'Evaluation of LAI-2000 for leaf area index monitoring in paddy rice'. *Field Crops Research*, vol. 99, no. 2-3, pp. 167-170.
- Tian, Y., Woodcock, C. E., Wang, Y., Privette, J. L., Shabanov, N. V., Zhou, L., Zhang, Y., Buermann, W., Dong, J., Veikkanen, B., Häme, T., Andersson, K., Ozdogan, M., Knyazikhin, Y. and Myneni, R. B. 2002. 'Multiscale analysis and validation of the MODIS LAI product: I. Uncertainty assessment'. *Remote Sensing of Environment*, vol. 83, no. 3, pp. 414-430.

- Verhoef, W. 1984. 'Light scattering by leaf layers with application to canopy reflectance modeling: The SAIL model'. *Remote Sensing of Environment*, vol. 16, no. 2, pp. 125-141.
- Verhoef, W. 2010. *RE: Discussion about the effect of PROSPECT parameters within the modelling of LAI*.
- Verhoef, W. and Bach, H. 2007. 'Coupled soil-leaf-canopy and atmosphere radiative transfer modeling to simulate hyperspectral multi-angular surface reflectance and TOA radiance data'. *Remote Sensing of Environment*, vol. 109, no. 2, pp. 166-182.
- Vermote, E. 2008. MOD09 (Surface Reflectance) User's Guide.
- Wang, F. and Huang, J. 2009. Narrow Band Ratio Vegetation Indices and Its relationships With Rice Agronomic Variables.
- Wang, Y., Tian, Y., Zhang, Y., El-Saleous, N., Knyazikhin, Y., Vermote, E. and Myneni, R. B. 2001. 'Investigation of product accuracy as a function of input and model uncertainties: Case study with SeaWiFS and MODIS LAI/FPAR algorithm'. *Remote Sensing of Environment*, vol. 78, no. 3, pp. 299-313.
- Weiss, M., Troufleau, D., Baret, F., Chauki, H., Prévot, L., Olioso, A., Bruguier, N. and Brisson, N. 2001. 'Coupling canopy functioning and radiative transfer models for remote sensing data assimilation'. *Agricultural and Forest Meteorology*, vol. 108, no. 2, pp. 113-128.
- Wu, X., Cheng, Q. and Mao, Z. Year. Validation of MOD15-LAI and MOD13 using in situ rice data. In: KULIGOWSKI, R. J., PARIHAR, J. S. & SAITO, G., eds., 2006 Goa, India. SPIE, 64111F-9.
- Xiao, X., Boles, S., Frohling, S., Li, C., Babu, J. Y., Salas, W. and Moore Iii, B. 2006. 'Mapping paddy rice agriculture in South and Southeast Asia using multi-temporal MODIS images'. *Remote Sensing of Environment*, vol. 100, no. 1, pp. 95-113.
- Xiao, X., Boles, S., Liu, J., Zhuang, D., Frohling, S., Li, C., Salas, W. and Moore Iii, B. 2005. 'Mapping paddy rice agriculture in southern China using multi-temporal MODIS images'. *Remote Sensing of Environment*, vol. 95, no. 4, pp. 480-492.
- Yang, W., Shabanov, N. V., Huang, D., Wang, W., Dickinson, R. E., Nemani, R. R., Knyazikhin, Y. and Myneni, R. B. 2006. 'Analysis of leaf area index products from combination of MODIS Terra and Aqua data'. *Remote Sensing of Environment*, vol. 104, no. 3, pp. 297-312.
- Yi, Y., Yang, D., Huang, J. and Chen, D. 2008. 'Evaluation of MODIS surface reflectance products for wheat leaf area index (LAI) retrieval'. *ISPRS Journal of Photogrammetry and Remote Sensing*, vol. 63, no. 6, pp. 661-677.
- Yongming, D., Qiang, L., Qing-Huo, L. and Liang-Fu, C. 2004. 'Estimate LAI of crops using airborne multi-angular data'. *IGARSS 2004. 2004 IEEE International Geoscience and Remote Sensing Symposium*, vol. 7, no., pp. 4477-4479 vol.7.

9. Appendices

Appendix A

Weekly values of LAI from *in situ* measurements and MODIS LAI/FPAR product

Plot	Week 1		Week 2		Week 3		Week 4		Week 5	
	Field	MODIS								
P01	3.02	1.68		2.01	4.89	2.58	5.45	3.59		2.79
P02	3.03				4.35		4.73			
P03	2.79	1.14		1.36	4.19	1.82	4.88	1.82		1.93
P04	1.11	0.48		0.64	3.27	0.69	3.08	0.68		0.73
P05	2.48	0.75		0.97	3.70	1.18	2.94	1.20		1.53
P06	2.37	0.91		1.11	3.99	1.41	3.73	1.52	4.90	1.72
P07	3.07	0.71		1.20	4.53	1.43	4.23	1.65		1.81
P08	1.96	0.72		1.24	3.80	1.65	4.15	1.96		2.17
P09	2.82	0.58		0.99	4.15	1.32	4.54	1.57		1.74
P10	2.79	0.78		1.34	4.29	1.78	4.63	2.12		2.34
P11	3.02	0.67		0.95	3.70	1.16	4.54	1.16		1.22
P12	1.47	0.39		0.67	3.65	0.87	3.58	0.87		0.96
P13	4.15	0.89		1.15	4.45	1.27	4.67	1.27	4.17	1.53
P14	3.55	0.57		0.80	4.29	0.80	4.97	0.92	5.21	1.14
P15	2.69	0.55		0.91	3.32	1.06	3.53	1.06	3.22	1.42
P16	1.46	1.45			4.30		4.15		4.38	
P17	2.32	0.81		1.38	3.02	1.73	3.84	1.61	3.80	2.30
P18	1.89	0.37		0.50	3.26	0.61	3.76	0.71	3.78	0.87
P19	3.44	0.31		0.49	3.73	0.60	4.15	0.61	5.17	0.85
P20	2.47	0.72		1.26	2.96	1.44	3.24	1.71	3.48	1.98
P21	1.44	0.43		0.61	3.01	0.61	3.07	0.78	2.76	0.87
P22	2.22	0.39		0.60	3.13	0.60	3.74	0.69	3.66	0.73
P23	2.11	0.45		0.66	3.54	0.74		0.83	3.89	0.88
P24	1.14	0.51		0.77	3.04	0.92		0.98	3.63	1.03
P25	1.63	0.37		0.49	2.76	0.49	2.70	0.69	3.31	0.86
P26	2.02	0.45		0.60	3.01	0.60	3.61	0.90	4.14	1.05

P27	3.22	0.32			2.83		3.10		3.08	
P28	3.73	1.27		1.85	3.18	2.63	3.86	2.73	3.90	3.60
P29	3.82	0.86		1.47	3.86	1.59	3.69	1.47	3.87	1.83
P30	4.08	1.17		1.73	3.78	2.53	4.43	2.78	3.96	3.64
P31	2.49	0.88	3.88	1.40	3.46	1.85	3.61	2.32		2.77
P32	2.52	0.94		1.50	3.71	1.99	4.29	2.48		2.97
P33	2.01	0.48		0.73	4.57	0.85	5.87	1.03		1.16
P34	3.43	0.57		0.84	4.20	1.05	4.88	1.16		1.39
P35	3.31	0.47		0.62	2.96	0.77	3.55	0.88	4.96	0.88
P36	3.59	0.50		0.70	3.19	0.90	3.68	1.10		1.10
P37	3.90	1.66	2.10	1.99	3.21	2.21	3.76	2.66		2.55
P38	3.10	1.32	3.28	1.52	3.72	1.48	4.45	1.77		1.71
P39		1.13	2.30	1.26	3.69	1.61	5.27	1.56		1.89
P40		1.51	3.14	1.81	5.04	2.09		3.10		2.28
Average	2.64	0.77	3.01	1.09	3.77	1.34	4.06	1.51	4.00	1.70

Appendix B

Weekly values of LAI from *in situ* measurements and SLC model.

Plot	Week 1		Week 2		Week 3		Week 4		Week 5	
	Field	SLC	Field	SLC	Field	SLC	Field	SLC	Field	SLC
P01	3.02	3.92			4.89	4.56	5.45	4.24		
P02	3.03	3.36			4.35	3.92	4.73	3.68		
P03	2.79	3.04			4.19	3.20	4.88	3.36		
P04	1.11	2.24			3.27	2.72	3.08	3.72		
P05	2.48	2.00			3.70	2.24	2.94	2.56		
P06	2.37	2.32			3.99	2.96	3.73	2.64	4.90	3.44
P07	3.07	2.16			4.53	2.88	4.23	2.88		
P08	1.96	2.16			3.80	2.88	4.15	2.88		
P09	2.82	2.08			4.15	2.72	4.54	2.72		
P10	2.79	2.08			4.29	2.72	4.63	2.72		
P11	3.02	1.84			3.70	2.88	4.54	2.96		
P12	1.47	1.84			3.65	2.88	3.58	2.96		
P13	4.15	3.28			4.45	3.92	4.67	3.68	4.17	4.00
P14	3.55	3.32			4.29	2.80	4.97	2.64	5.21	3.28
P15	2.69	2.48			3.32	2.80	3.53	3.20	3.22	3.44
P16	1.46	1.60			4.30	2.24	4.15	3.20	4.38	2.64
P17	2.32	2.48			3.02	2.80	3.84	3.20	3.80	3.44
P18	1.89	2.00			3.26	1.76	3.76	1.76	3.78	2.40
P19	3.44	1.60			3.73	2.24	4.15	3.20	5.17	2.64
P20	2.47	2.24			2.96	2.32	3.24	2.48	3.48	3.60
P21	1.44	1.84			3.01	2.32	3.07	2.24	2.76	3.04
P22	2.22	2.16			3.13	2.72	3.74	2.72	3.66	3.36
P23	2.11	1.76			3.54	2.16			3.89	2.00
P24	1.14	1.92			3.04	2.88			3.63	2.80
P25	1.63	2.08			2.76	2.08	2.70	1.84	3.31	1.76
P26	2.02	2.00			3.01	2.08	3.61	2.48	4.14	2.80
P27	3.22	2.40			2.83	2.32	3.10	2.24	3.08	2.00
P28	3.73	2.40			3.18	2.32	3.86	2.24	3.90	2.00

P29	3.82	2.24			3.86	4.00	3.69	3.68	3.87	3.92
P30	4.08	2.24			3.78	3.12	4.43	2.96	3.96	3.84
P31	2.49	1.68	3.88	2.32	3.46	2.88	3.61	2.72		
P32	2.52	2.24			3.71	2.88	4.29	2.96		
P33	2.01	2.16			4.57	3.12	5.87	2.88		
P34	3.43	1.84			4.20	2.40	4.88	2.00		
P35	3.31	2.16			2.96	2.96	3.55	2.56	4.96	2.96
P36	3.59	2.16			3.19	2.96	3.68	2.56		
P37	3.90	3.36	2.10	3.28	3.21	4.16	3.76	3.68		
P38	3.10	2.56	3.28	3.60	3.72	2.40	4.45	3.20		
P39			2.30	3.12	3.69	4.00	5.27	3.84		
P40			3.14	3.44	5.04	3.76				
Average	2.64	2.30	3.01	3.15	3.77	2.87	4.06	2.90	4.00	2.97